



Multifunctional Metal-Organic Frameworks: from Academia to Industrial Applications

Journal:	<i>Chemical Society Reviews</i>
Manuscript ID:	CS-SYN-04-2015-000307.R2
Article Type:	Review Article
Date Submitted by the Author:	17-Jun-2015
Complete List of Authors:	Silva, Patrícia; University of Aveiro, Department of chemistry, CICECO Vilela, Sérgio; University of Aveiro, Department of Chemistry, CICECO Tome, Joao; University of Aveiro, Department of Chemistry Almeida Paz, Filipe; University of Aveiro, Department of Chemistry, CICECO

Review
CS-SYN-04-2015-000307

Multifunctional Metal-Organic Frameworks: from Academia to Industrial Applications

Patrícia Silva,^{[a]§} Sérgio M. F. Vilela,^{[a,b]§} João P. C. Tomé^[b,c]
and Filipe A. Almeida Paz*^[a]

§ These authors contributed equally to the present manuscript

A contribution from

^[a] Department of Chemistry, CICECO – Aveiro Institute of Materials,
University of Aveiro, Campus Universitário de Santiago, 3810-193 Aveiro, Portugal

^[b] Department of Chemistry, QOPNA, University of Aveiro,
Campus Universitário de Santiago, 3810-193 Aveiro, Portugal

^[c] Department of Organic and Macromolecular Chemistry, Ghent University, B-9000
Ghent, Belgium

Corresponding author:
E-mail filipe.paz@ua.pt
Telephone: +351 234370200, Extension 23553
Fax: +351 234370084

Abstract

After three decades of intense and fundamental research on Metal-Organic Frameworks (MOFs), is there anything left to say or to explain? The synthesis and properties of MOFs have already been comprehensively described elsewhere. It is time, however, to prove the nature of their true usability: technological applications based on these extended materials require development and implementation as a natural consequence of the up-to-know intensive research focused at their design and preparation. The current large number of reviews on MOFs emphasizes practical strategies to develop novel networks with varied crystal size, shape and topology, being mainly devoted to academic concerns. The present survey intends to push the boundaries and summarise the state-of-the-art on the preparation of promising (multi)functional MOFs in worldwide laboratories and their use as materials for industrial implementation. This review starts, on the one hand, to describe several tools and striking examples of remarkable and recent (multi)functional MOFs exhibiting outstanding properties (*e.g.*, in gas adsorption and separation, selective sorption of harmful compounds, heterogeneous catalysis, luminescence and corrosion protectants). On the other hand, and in a second part, it intends to use these examples of MOFs to incite scientists to move towards the transference of knowledge from the laboratories to the industry. Within this context, we exhaustively review the many efforts of several worldwide commercial companies to bring functional MOFs towards the daily use, analysing the various patents and applications reported to date. Overall, this review goes from the very basic concepts of functional MOF engineering and preparation ending up in their industrial production in large scale and direct applications in society.

Table of Contents

1 – Introduction	4
2 – Creating and Improving	
2.1 – Synthesis.....	5
2.2 – Applicability	5
2.2.1 – Hydrogen and Methane Storage	6
2.2.2 – CO ₂ Capture.....	8
2.2.3 – Removal of harmful and toxic chemicals	9
2.2.4 – Heterogeneous catalysis.....	11
2.2.5 – Luminescence	13
2.2.6 – Metal corrosion inhibition.....	14
3 – MOF production at the industrial scale	15
3.1 – Financial and environmental viability.....	15
3.2 – Market Opportunities and Commercial applications	16
3.2.1 – Examples of large-scale production of MOFs	16
3.2.2 – Industrial property	17
3.2.3 – Transport and Oleochemical industry.....	17
3.2.4 – Textile industry.....	19
3.2.5 – Respiratory systems	20
3.2.6 – Food packaging.....	20
4 – Final Remarks	21
5 – List of Abbreviations	22
6 – Acknowledgements	23
7 – References	24

1 - Introduction

Over the past three decades, new materials based on Metal-Organic Frameworks (MOFs) have been reported almost on a daily basis. Nonetheless, MOF terminology usually implies some ambiguity or confusion with the term Coordination Polymer (CP). We thus direct the readers to the hierarchical definition of CPs and MOFs recently proposed by Batten.¹ Beyond the academic interest in obtaining rigorous definitions,² the distinction between these two types of structures is of great interest because MOFs usually exhibit higher thermal stability, permanent porosity and structural robustness when compared with polymers in general. Typically, strong interatomic bonds are not confined to a single plane: self-assembly polymerization is carried out by metal ions or clusters and rigid organic molecules joined together by coordinative bonds, leading to highly crystalline materials infinitely drawn-out into 3D structures.^{1,3} The emergence of MOFs is often considered as a way to mimic inorganic materials as, for instance, zeolites. This is actually an oversimplification of what was a natural consequence in the design and preparation of extended (hybrid) materials with permanent microporosity.⁴ Unlike zeolites, MOFs permit a close control of the shape, size and functionalization of the pores.⁵

The best/ideal compound/material is easy to prepare, stable and simple to use. In a sense, MOFs can easily address these needs: synthetic design principles are simple in nature and solely based on a judicious initial choice of ligands and metal centres, which then self-assemble in the solid state under specific synthetic conditions. The overwhelming variety of such basic units guarantees an endless universe of hybrid organic-inorganic combinations.⁶ A search in the literature reveals, however, that there are some recurrent structural motifs in MOF preparation as an attempt to predict their architectures.⁷⁻⁸

Given that the universe of MOFs can accommodate almost all cations, literature presents many examples on the use of alkaline earth and transition metals or even lanthanides.^{7,9} Concerning the organic molecules, which act as bridges between those metal ions, multidentate molecules with one or more *N*- or *O*-donor atoms are typically used. Common ligands include molecules with pyridyl and cyano groups, carboxylates, phosphonates, crown ethers, and polyamines (in particular those derived from benzene, imidazole and oxalic acid).¹⁰ In a sense, this type of molecular manipulation was the way that chemists found to prove the concept of chemical modification of MOFs and the concomitant prediction of network topologies alongside with their dimensionality, size and shape control. For instance, aromatic molecules are often used when some rigidity or geometrically defined clusters are sought.

The incorporation of functionality into the linkers by means of the use of a certain reactive group, or a chiral or a redox centre, results in the achievement of an aimed characteristic throughout the bulk material.³ Traditional organic synthesis or, in alternative, *in situ* preparation methods play a major role when creating novel linkers or modifying those molecules that are commercially available. On the other hand, the dimensionality of the final product is also related with the coordination geometry: electronic configuration, coordination modes, size or hardness of the metal centre influence the final framework topology.¹¹⁻¹³ All in all, the choice of these primary building units may influence the pore size of a given material, and it may affect energy conversion performances, conductivity or catalytic behaviour, among many other factors.³

Some of the most striking MOF architectures that have influenced worldwide research can be found in the research of the Yaghi, O'Keeffe or Férey groups, in materials like MOF-5 or the MIL-*n* series.¹⁰ MOF-5 is the Yaghi's most popular framework (Figure 1, as IRMOF-1), largely pointed as the first architecture that gave birth to the reticular chemistry concept in MOFs. Isotypical topologies achieved from different organic linkers (by changing the molecule length, substituting groups, derivatization, functionalization of the pores)¹⁴ are, in fact, based in the same basic structural design. For instance, the first 16 derivatives of MOF-5 have the same framework topology built of Zn₄O clusters connected by different linear dicarboxylates into cubic lattices (Figure 1). The importance of such families of structures relies on the systematic creation of compounds having different pore sizes with the concomitant tuning of framework properties. Thus, it is not surprising that porosity has been the MOF subfield that has evolved the most in the last years. MOFs have been largely studied for their gas-storage and separation properties, catalytic performance and host-guest exchange. The percentage of truly functional MOFs which can be used in materials science and devices is, however, scarce to this date. This is because most of the research efforts have been for a long period essentially focused at the isolation of solely novel architectures.

→ Insert Figure 1 ←

Nowadays cutting-edge research based on MOFs is strongly related to the production of functional devices, mainly motivated by their outstanding surface areas and possibility to be prepared with readily available and cheap reactants. Synthetic approaches have been fine-tuned over the years for each material and their structures fully elucidated. Researchers are currently able to develop with great success MOF materials scaling up the basic science into the realm of applications. Scientists are, in this way, much more focused in developing solutions for the real world problems and have clearly favoured clean energy technologies (with particular emphasis on purification, storage, and transport of gases).^{10, 15} MOF investigation is also spread over new fields such as biomedicine,¹⁶ magnetism,¹⁷⁻¹⁸ conductivity,^{10, 19} fabrication of membranes,²⁰ or light-based devices.²¹⁻²⁴

This review does not intend to be not an exhaustive survey literature describing minutely the basic concepts, primary building blocks (PBUs, *i.e.*, organic linkers and metallic centres), topologies and structural features as well as all the intrinsic properties of MOFs. For this purpose there are several interesting dedicated reviews reported over the last few years, to which we direct the reader.^{3, 7, 10, 25-35} Herein, we intend to provide: i) some highlights of the synthetic methodologies summarizing their main advantages and disadvantages; ii) striking examples of functional MOFs prepared in worldwide laboratories (most of them located in academia) which can be strong candidates for potential industrial applications and that serve as remarkable examples of the great potential usefulness of these materials; and iii) a detailed summary of the state-of-the-art towards the preparation of MOF-based devices for industrial implementation, which includes the many efforts of industry to patent and commercialize these compounds. Overall, this review aims to go from the basic academia laboratory to the direct application of a MOF material in our daily life, showing that these compounds can indeed be much more than intellectual exercises of an educated mind.

2 - Creating and Improving

2.1 - Synthesis

The process to produce a MOF starts with a careful selection of the PBUs. A countless number of architectures have been isolated combining *N*- or *O*-donor molecules with several elements of the periodic table (mainly transition metals and, not so commonly until recent years, lanthanides).^{7, 24, 27} The selected PBUs play, undoubtedly, a very important role concerning the final structure and properties of the MOF. However, several other synthetic parameters (*e.g.*, pressure, solvent, pH, reaction time and temperature) and approaches must also be taken into account.^{7, 18, 36-37} Depending on the final purpose, multidimensional MOFs may be prepared employing several and distinct synthetic methodologies: we note that some are faster and with low energy consumption, being more attractive for industrial purposes.

The possibility to prepare the desired materials as large single-crystals is, very often, a difficult but important task, which influences which method is ultimately selected. In many cases, depending on the intended final aim, a wide range of methods could be used for the same material (for example, when the scientist intends not only to isolate large single crystals but also to reduce crystallite size for applications). Table 1 summarizes the main advantages and disadvantages of each synthetic methodology.

→ Insert Table 1 ←

2.2 - Applicability

The presence of organic and inorganic PBUs in the structure of MOFs allows their potential application in several and distinct fields due to the improved properties resulting from the symbiotic combination of these two different components:

- i) Porosity. Undoubtedly, the most desired property in order to allow the accommodation of chemical entities as, for instance, in the storage of energy-relevant gases (*e.g.*, H₂, CH₄),⁶⁸⁻⁶⁹ capture of CO₂,⁷⁰ removal of toxic gas molecules⁷¹ and inclusion of biologically active species.¹⁶ In this context, a great evolution have been observed concerning the pore/cage sizes (Figure 2) leading to the isolation of several highly porous MOF structures over the years (Figure 3);
- ii) Catalytic activity. To convert chemical species, some of them dangerous for humans and the environment, into others which are significantly more safe or with industrial interest;⁷²
- iii) Luminescence. A phenomenon which results from the emission of radiation from vibrationally or electronically excited species;^{21, 23}
- iv) Magnetism, which depends on the nature and spatial relation of both metallic centres and organic linkers, and the organizational level originated by the ligand-metal coordination;¹⁸
- v) Electrochemistry, involving the storage or transference of electrons at the electrode-electrolyte interface. MOFs are potential materials to be used in the positive electrode in Li-based batteries and as corrosion inhibitors of metal surfaces.⁷³⁻⁷⁵

→ Insert Figure 2 ←

→ Insert Figure 3 ←

2.2.1 - Hydrogen and Methane Storage

One of the main challenges for chemists in the 21st century concerns energy storage. On the one hand, hydrogen (H₂) appears as an environmentally friendly energy carrier and clean fuel. On the other, methane (CH₄), a component of natural gas, seems also to be an attractive fuel because of its abundance and burning process, which is relatively clean. In this way, both H₂ and CH₄ are excellent and realistic alternatives to the more common fossil fuels. The pressing need to store and use them as fuels in a cheap, safe and convenient way is thus a great requirement and, simultaneously, a challenging task. Keeping that in mind, a considerable amount of research comprising the discovery of suitable MOF materials has been reported aiming at facilitating their storage, as for instance, in automobiles, while fulfilling the published requirements. The U.S. Department of Energy (DOE) published recently the following storage target values: for H₂, at an operating temperature of -40 to -60 °C and amenable pressures (< 100 bar), a target of 5.5 wt% and 40 g L⁻¹ by 2015; for CH₄ the target is 263 (STP) cm³ cm⁻³ (25 °C, 35 bar) (*Note*: STP means standard temperature and pressure) which, we note, is a significantly higher value than the previous reported one (180 (STP) cm³ cm⁻³).^{68-69, 77}

Because H₂ is a viable energy source to replace common fossil combustibles (which are the main contributors for the greenhouse effect), several research groups have dedicated their efforts to design and produce porous materials with capacity to store this gas in a safe and cheap manner and, consequently, use it as an energy source in vehicles. Hydrogen storage requires specific conditions:

- i) very high pressure gas;
- ii) liquid hydrogen;
- iii) intercalating of H₂ in metals;
- iv) porous materials.⁷⁸

The hydrogen storage capacity of several known families of MOFs as, for instance, IRMOFs,⁷⁹ MILs,⁸⁰ ZIFs,⁸¹ NOTTs,⁸² PCNs⁸³ and SNUs⁸⁴ have been extensively studied. Both small pore sizes (in order to allow the interaction of H₂ with the wall of the MOF) and the incorporation of coordinatively unsaturated metal centres (to bind H₂) are two important requirements to retain H₂.^{68, 85-87} Nevertheless, other strategies have been adopted to improve H₂ uptake: i) post-synthetic processes;⁸⁸⁻⁸⁹ ii) variation in the pore features;^{82, 90-91} iii) use of mixed crystals of known MOF materials prepared in different solvents;⁹² and iv) the use of polarized organic linkers.⁸⁵

Hydrogen adsorption properties in MOFs were firstly reported for the iconic MOF-5. This material is able to adsorb up to 4.5 wt% of H₂ at cryogenic conditions and 1 bar of pressure.⁹³ In 2007, Belof *et al.*⁹⁴ studied the mechanism of H₂ adsorption in porous MOFs to evaluate how this gas binds in two indium frameworks: [In₃O(C₈O₄H₄)₃(H₂O)_{1.5}(C₃N₂H₃)(C₃N₂H₄)_{0.5}]·DMF·0.5(CH₃CN) and [In₃O(C₁₆N₂O₈H₆)_{1.5}(H₂O)₃](H₂O)₃(NO₃), initially prepared by Liu and collaborators.⁹⁵ It was discovered that: i) the MOF material, alongside its high surface area, has a large number of interdigitated pores; ii) open frameworks with low density MOFs allow H₂ adsorption due to H₂-H₂ interactions which occur in the middle of the channels; and iii) the inner surface should have local polar groups in order to promote MOF-H₂ interactions. This last characteristic is directly attributed to the properties of the organic PBUs. To support that, it was shown that the structure of Liu *et al.* containing an organic spacer with an N=N connection provides significantly more MOF-H₂ interaction sites.

Mulfort and co-workers described a strategy to improve H₂ uptake,⁸⁸ with the work consisting in a post-synthesis procedure in order to convert pendent alcohol moieties to metal alkoxides. The as-prepared porous DO-MOF material (having in its structure Zn²⁺ metallic centres and two different organic ligands (a tetracarboxylate and a bipyridine molecule) was added to a mixture composed of THF, to replace the guest solvent molecules of DMF, and an excess of Li⁺[O(CH₃)₃] in CH₃CN/THF. The H₂ uptake capacity of the as-prepared DO-MOF, as well as the DO-MOF-Li, were investigated and the results suggest that at 77 K (1 atm), the DO-MOF-Li material has higher H₂ uptake (1.32 wt%) than the original DO-MOF (1.23 wt%).

Recently, composite materials and core-shell MOF nanocrystals have been produced to enhance hydrogen storage.⁹⁶⁻⁹⁹ Li *et al.* prepared the Pd@HKUST-1 composite material by using a facile reactive seeding methodology: Pd nanocube crystals work as seed sites for MOF growth (Figure 4).⁹⁶ Nanoparticles were coated through the use of a solution of the precursors (trimesic acid and Cu²⁺ cations) of HKUST-1 and ethanol. Hydrogen pressure-composition isotherms and solid-state deuterium nuclear magnetic resonance (NMR) experiments suggest that Pd nanocubes coated with HKUST-1 MOF material exhibit two times more hydrogen storage capacity than the uncoated nanocrystals. Core-shell nanoparticles were isolated by Ren and collaborators by incorporation of the microporous UiO-66 into the mesoporous MIL-101 material (working as seeds), with both MOFs retaining their native morphology.⁹⁹ To the mixture for the preparation of UiO66 (containing ZrCl₄, 1,4-benzenedicarboxylic acid in DMF and formic acid) the seeding particles of MIL-101 were added in order to originate the hybrid nano-sized MIL-101@UiO-66 material. The capacity of the core-shell MIL-101@UiO-66 for H₂ uptake increased *ca.* 26% and 60% when compared with the phase-pure MIL-101 and UiO-66, respectively.

→ Insert Figure 4 ←

Concerning CH₄, it was reported that zeolites exhibit uptakes below 100 (STP) cm³ cm⁻³ and porous carbon materials are capable of storing CH₄ in the 50-160 (STP) cm³ cm⁻³ range.¹⁰⁰⁻¹⁰¹ Despite the good performance of these families of materials, particularly porous carbon materials, towards the adsorption of CH₄ the reported values still fall outside the main target imposed by the U.S. DOE (263 (STP) cm³ cm⁻³). One inconvenience in the storage of CH₄ is based on its low energy density. This leads to the need to store this gas either at very high pressures (200-300 bar for compressed methane) or as a liquid (112 K for liquefied methane) for usage in, for instance, vehicles.¹⁰²⁻¹⁰⁴ The storage of methane in porous materials as in MOFs arises, therefore, as a promising alternative to achieve the ambitious U.S. DOE targets under moderate pressures (35-65 bar) and ambient temperature.^{103, 105} In 2000, Kitagawa *et al.* reported the preparation of [CuSiF₆(4,4'-bpy)], a new inorganic-organic hybrid material potentially able to effectively adsorb methane.¹⁰⁶ Since then, dozens of MOFs have been prepared with good storage capacity, of which we emphasize HKUST-1,¹⁰⁷ MIL-101,¹⁰⁷ USTA-20,¹⁰⁸ NU-111,¹⁰⁹ NU-125,¹¹⁰ NOTT-122¹¹¹ and PCN-14.¹¹²

Peng and collaborators described an interesting work reporting the ability of six well-known MOFs (NU-111, NU-125, UTSA-20, PCN-14, Ni-MOF-74 (Ni-CPO-27) and HKUST-1) in CH₄ uptake (Figure 5).⁷⁷ Results were very promising: although Ni-MOF-74 can adsorb a high amount of CH₄, the commercially available in the gram scale HKUST-1 exceeds any value reported to date. At ambient temperature the volumetric CH₄ uptake for this material is about 230 cm³ cm⁻³ at 35 bar and 270 cm³ cm⁻³ at 65 bar. These values reach the new volumetric target recently set by the DOE if the packing efficiency

loss is ignored. Despite these excellent results, other issues remain as, for instance, the cost and the chemical stability of these materials.

→ Insert Figure 5 ←

Yaghi's research group prepared two aluminum-based MOFs, coined as MOF-519 and MOF-520,¹¹³ with permanent porosity. The former adsorbs 200 and 279 cm³ cm⁻³ of CH₄ at 298 K and 35 and 80 bar, respectively, while the latter has a volumetric capacity of 162 and 231 cm³ cm⁻³ under the same conditions. Additionally, MOF-519 possesses working capacities of 151 and 230 cm³ cm⁻³ at 35 and 80 bar, respectively, with the first value rivalling with the well-known HKUST-1 material, and the second one being a world record compared with all the top performing MOF materials under the same conditions (Figure 6).

→ Insert Figure 6 ←

2.2.2 - CO₂ Capture

CO₂ is the major responsible of the greenhouse effect. It is reported that during the last half century the concentration of CO₂ in the atmosphere increased from about 310 to over 380 ppm, being expected to achieve 550 ppm by 2050 even if CO₂ emissions stabilize in the next four decades.¹¹⁴⁻¹¹⁶ These values are a consequence of the intense CO₂ release from industries and from the combustion of fossil combustibles. Because of this, several strategies have been developed for the sequestration/reduction of CO₂ of which we emphasize: i) the replacement of common fossil combustibles by environmentally friendly H₂ and CH₄; ii) preparation of porous structures with high affinity towards CO₂ so to avoid its release to the atmosphere. The U.S. DOE established a program envisaging the retention of 90% of CO₂ emissions *via* the post-combustion process allowing an increase in the cost of electricity no more than 35% by 2020.¹¹⁶ The reduction of CO₂ emissions comprises three main separation procedures, such as separation from fuel gas, power plant combustion flows and natural gas sources.¹¹⁷

Porous MOF-based materials have emerged as a new type of functional CO₂ adsorbents.^{20, 70, 114, 118} These compounds should have some specific characteristics and requirements to be used as efficient CO₂ adsorbents: i) porosity, with good accessibility to the channels; ii) thermal stability; iii) the presence of organic ligands derived from nitrogen-containing heterocycles and/or the iv) existence of functional groups (*e.g.*, -NH₂ or -OH groups) in the pores to interact with CO₂, and boost adsorption; v) insertion of metal ions; and vi) the presence of open metal sites.^{111, 119-122} Alongside these features, the decrease in the production cost of MOFs is another important requirement envisaging their possible industrial availability.

A large number of reports have emerged describing the ability of MOFs to retain remarkable amounts of CO₂ in their channels: NOTT-122 (9.0 mmol g⁻¹),¹¹¹ HKUST-1 (10.7 mmol g⁻¹),¹²³ MOF-5 (21.7 mmol g⁻¹),¹²³ MOF-117 (33.5 mmol g⁻¹),¹²³ MIL-100(Cr) (18.0 mmol g⁻¹),¹²⁴ MIL-101(Cr) (40.0 mmol g⁻¹),¹²⁴ NU-100 (46.4 mmol g⁻¹),¹²⁵ UMCM-1 (23.5 mmol g⁻¹),¹²⁶ MOF-200 (54.5 mmol g⁻¹)¹²⁷ and MOF-210 (54.5 mmol g⁻¹).¹²⁷

Despite the high affinity of some porous MOF materials toward CO₂, the capacity to separate the gas from a mixture of gases is not, very often, investigated. Nevertheless, some reports have emerged describing the selective adsorption of CO₂ over other gases (*i.e.*, N₂, CH₄, O₂, C₂H₂ or CO), some of which even comprise binary (*e.g.*, CO₂/CO, CO₂/N₂ or CO₂/CH₄) and ternary (CO₂/N₂/CH₄, CO₂/N₂/H₂O or CO₂/N₂/O₂) gas mixtures.^{119-120, 128-135} Wang *et al.* reported two porous zeolite-type imidazolate frameworks, coined as ZIF-95 and ZIF-100, possessing complex cages with 264 vertices and constructed from about 7524 atoms.¹²⁸ After breakthrough experiments it was discovered that these ZIFs selectively adsorb CO₂ from mixtures of CO₂/CH₄, CO₂/CO and CO₂/N₂ (50:50 v/v). The average selectivity of CO₂ over CH₄, CO and N₂ are in the order of 4.3:1, 11.4:1 and 18.0:1, respectively, for ZIF-95, and 5.9:1, 17.3:1 and 25:1, respectively, for ZIF-100. Britt and co-workers studied the known porous Mg-MOF-74

material in CO₂ separation processes.¹²⁹ Breakthrough experiments using a mixture of CH₄/CO₂ (4:1) showed that CO₂ is substantially more adsorbed than CH₄ with a dynamic capacity of 8.9 wt% CO₂ uptake (Figure 7). It was further reported that CO₂ can be easily released from Mg-MOF-74 at lower temperatures.

→ Insert Figure 7 ←

More recently, Navarro's research group designed and prepared three novel nickel face-cubic centered functional MOFs: [Ni₈(OH)₄(H₂O)₂(BDP)₆], [Ni₈(OH)₄(H₂O)₂(BDP_OH)₆] and [Ni₈(OH)₄(H₂O)₂(BDP_NH₂)₆].¹¹⁹ All materials were treated with KOH leading to the post-synthetically modified K[Ni₈(OH)₅(EtO)(H₂O)₂(BDP)_{5.5}], K₃[Ni₈(OH)₃(EtO)(H₂O)₆(BDP_O)₅] and K[Ni₈(OH)₅(EtO)(H₂O)₂(BDP_NH₂)_{5.5}] networks retaining the parent framework topology. Dynamic adsorption measurements (*i.e.*, variable temperature pulse gas chromatography and separation breakthrough experiments) suggest that the incorporation of K⁺ cations into the frameworks leads to a higher interaction of the structures with CO₂ than N₂, particularly for K₃[Ni₈(OH)₃(EtO)(H₂O)₆(BDP_O)₅]. This material also exhibits a high degree of recyclability, retaining activity during at least ten successive CO₂ capture cycles.

To improve the selective adsorption capacity towards CO₂ envisaging, at the same time, a possible application in industry, MOFs have been employed in the production of composites¹³⁶⁻¹³⁷ and membranes.¹³⁸⁻¹⁴³ The Ag@MIL-101 porous material, with different Ag loadings, was prepared by Liu *et al.*¹³⁷ via a simple impregnation-reduction methodology immobilizing Ag nanoparticles into the cages of MIL-101(Cr). This material exhibits outstanding bifunctionality: i) on the one hand, Ag@MIL-101 is capable of retaining CO₂ in its porous structure; ii) on the other hand, CO₂ is converted into compounds with carboxylic acid groups through C-H bond activation of the terminal alkynes. This is a low-energy consumption process (reactions occur at mild conditions: 50 °C and 1 atm of CO₂) and Ag@MIL-101 acts as a truly heterogeneous catalyst, being easily recovered by centrifugation and reused in several consecutive cycles with good catalytic activity and high stability in the carboxylation of terminal alkynes. Because of all these interesting and rare features, Ag@MIL-101 can find applications in both synthetic and industrial chemistry, medicine and also for the reduction of the greenhouse CO₂ present in the environment.

The research group of Gascon prepared mixed matrix membrane (MMMs) based on the NH₂-MIL-53(Al) MOF material as a promising alternative for CO₂ removal from natural gas.¹⁴¹ MMMs were produced by dispersing NH₂-MIL-53(Al), with MOF loadings up to 25 wt% in polyimide. The final membranes were quantitatively characterized by using tomographic focused ion beam scanning electron microscopy (FIB-SEM, Figure 8). The performance of the NH₂-MIL-53(Al)-based membranes were investigated in the capture of CO₂ using a CO₂:CH₄ (1:1) gas mixture (Figure 9). Results suggest that the membrane with a 25 wt% MOF has an increase of 50% in the CO₂ permeability when compared with the MOF-free membrane, while, remarkably, retaining the separation selectivity and, additionally, improving its mechanical stability.

→ Insert Figure 8 ←

→ Insert Figure 9 ←

2.2.3 - Removal of harmful and toxic chemicals

The release of harmful and toxic chemicals into the environment is an international concern that has recently attracted the attention of worldwide scientists. Numerous studies using porous materials have been performed in the last few years with MOF compounds emerging as excellent alternatives towards the removal of those chemical species.^{71, 144}

The most common hazardous molecules present in our indoor and outdoor environments comprise CO_x , NO_x , SO_x , H_2S , NH_3 , PH_3 , volatile organic compounds (VOCs, including benzene, toluene, xylenes, cyclohexane, dichloromethane, chloroform, acetone and methanol: solvents used routinely in laboratory practices), nitrogen-containing compounds (NCCs, *i.e.*, pyridine, imidazole and amines), sulphur-containing compounds (SCCs, *i.e.*, ethyl mercaptan, dimethyl sulfide, thiophene and mustard gas), pharmaceutical and personal care products (PPCPs, *e.g.*, removal of naproxen and clofibric acid from water), nerve agents (*e.g.*, sarin), among others.¹⁴⁵⁻¹⁵⁷ Exposure to these families of harmful and toxic compounds (normally emitted in large quantities as, for example, from industrial chemical processes, combustion of natural gas, deliberate emission of chemical warfare species, use of fungicides in agriculture practices) may lead to serious environment and human health problems, such as: i) severe disorder of the respiratory system;¹⁵⁸ ii) sensory irritation symptoms;¹⁵⁹ iii) carcinogenicity;¹⁵⁸ iv) endocrine disruptions leading to possible change in the hormonal actions;¹⁴⁷ v) disruption of the nervous system which may cause death in minutes (use of sarin gas in chemical warfare);¹⁵⁴ and vi) formation of photochemical smog and acid rain (caused by the emission of SO_x and NO_x species).¹⁵⁵ To tackle these phenomena, several research groups have reported the development and use of MOF structures with potential to interact, and consequently remove, many hazardous chemicals.

Britt *et al.* studied the performance of six MOFs and IRMOFs (MOF-5, IRMOF-3, MOF-74, MOF-177, MOF-199 and IRMOF-62) as selective adsorbents of eight harmful gases (sulphur dioxide, ammonia, chlorine, tetrahydrothiophene, benzene, dichloromethane, ethylene oxide and carbon monoxide).¹⁴⁵ Kinetic breakthrough experiments were performed for all gases using each MOF as the adsorbent. Data were compared with a sample of Calgon BPL carbon (a common activated carbon used in several doped forms for many protective applications). MOF-74 and MOF-199 (both with coordinatively unsaturated metal sites) and IRMOF-3 (with $-\text{NH}_2$ groups) showed a great capacity in the adsorption of harmful gases. MOF-199 reveals also a good efficiency equal or greater than Calgon BPL carbon against all tested gases and vapours.

Hasan and collaborators investigated the adsorptive removal of two PPCPs (naproxen and clofibric acid) from water using MIL-101 and MIL-100-Fe.¹⁴⁷ As in the previous study, the performance of the MOFs were compared with that of active carbons. Results revealed that the removal efficiency decreases in the order of MIL-101 > MIL-100-Fe > activated carbon concerning both the adsorption rate and the adsorption capacity. In this context, the investigated MOF materials showed great potential to be used as adsorbents for the removal of PPCPs from contaminated water, much more than the more commonly employed activated carbons.

Navarro's research group reported the preparation of a robust and hydrophobic MOF-5 type material formulated as $[\text{Zn}_4(\mu_4\text{-O})(\mu_4\text{-4-carboxy-3,5-dimethyl-4-carboxy-pyrazolato})_3]$ (Figure 10a), designed specifically for the capture of nerve agents and mustard gas analogues (Figure 10b).¹⁵² This MOF has a remarkable thermal, mechanical and chemical stability, with these being required features for useful practical applications (see the introductory section of the present review). Dynamic variable-temperature pulse gas chromatography measurements were performed using the analogue compounds diisopropylfluorophosphonate (DIFP) and diethylsulfide (DES) of isopropylmethylfluorophosphate (IMFP, Sarin nerve gas) and bis(2-chloroethyl)sulfide (BCES, mustard vesicant gas), respectively, at different temperatures (Figures 10c and 10d). Chromatograms revealed good affinity between DIFP and DES with the MOF material, mainly at lower temperatures. It was further discovered that because of its hydrophobic character, this material has the ability to sustain adverse usage conditions in air/gas purification equipment (the features found for $[\text{Zn}_4(\mu_4\text{-O})(\mu_4\text{-4-carboxy-3,5-dimethyl-4-carboxy-pyrazolato})_3]$, even surpass the well-known $[\text{Cu}_3(\text{btc})_2]$, with the registered performance approaching that of the carbon molecular sieve adsorbent Carboxen).

→ Insert Figure 10 ←

With the perspective to convert laboratory essays by using bulk crystalline powdered MOFs into MOF-based composites or devices for practical applications, a number of studies have been reported in recent years, namely those concerning composites¹⁶⁰ and thin films¹⁶¹⁻¹⁶⁵ for the detection of hazardous chemicals. Ahmed *et al.* prepared the porous MIL-101 in the presence of graphite oxide (GO) to produce adsorbent GO/MIL-101 composites for the removal of NCCs and SCCs [*i.e.*, benzothiophene (BT),

quinolone (QUI) and indole (IND)]. It was observed that: i) the surface area of the GO/MIL-101 composites strongly depends on the amount of GO used, with only 0.25% of GO improving considerably the BET surface area of MIL-101 (from 3155 to 3858 m² g⁻¹); ii) the adsorption capacities of the GO/MIL-101 composites towards NCCs and SCCs were improved when compared with the GO and MIL-101 standalone starting adsorbents; and iii) GO/MIL-101 composites (having 0.25% of GO) can be reused after regeneration without noticeable degradation on the adsorption performance.

Thin films of [Cu₃(BTC)₂(H₂O)₃] \cdot xH₂O and [Zn₄O(BDC)₃] were grown from COOH-terminated self-assembled monolayers on the top of gold electrodes of quartz crystal microbalances or silicon microcantilevers (both electrochemical devices were used in chemical sensing).¹⁶⁵ This interesting work, reported by Yamagiwa *et al.*, shows the detection of several VOCs (ethanol, acetone, toluene, *n*-octane, *n*-octanol, *n*-hexane, *n*-hexanol, *n*-heptane, *n*-heptanol, *o*-, *m*- and *p*-xylene) by the MOF layers that act as effective concentrators of the gases. Adsorption/desorption processes were monitored by the frequency changes of the weight-detectable sensors coated within the MOF materials (Figure 11). Both MOFs showed high sensitivity and selectivity for VOC sensing and, depending of the employed material in the coating of the sensor, the sensitivities were found to vary according to the VOC. In short, weight-detectable sensors coated with MOFs have great potential for the preparation of sensing platforms to produce artificial electronic nose systems.

→ Insert Figure 11 ←

2.2.4 - Heterogeneous catalysis

Catalysis is, undoubtedly, a research field with great interest and continuous importance in the realm of MOFs. The quest for solid and recyclable catalytic compounds has marked large periods in scientific research, with the recyclability of a heterogeneous catalyst being one of the main pursued objectives because of both economic and environmental reasons.

Zeolites are the most common materials used in industrial heterogeneous catalysis. The preparation of catalytic-active MOFs does not aim to replace zeolite materials, but, on the contrary, to fill a number of important gaps never achieved to date for these materials, as for instance, in enantioselective heterogeneous catalysis. Because several MOFs have been shown to be interesting, stable solid materials in many organic solvents, their recover after catalytic essays can be easily performed. For a MOF to have excellent catalytic behaviour it is absolutely imperative the presence of active catalytic sites arising from the metal or organic molecules (or both). Therefore, the capacity to insert functional groups into porous MOFs and the presence of well-defined channels (allowing size and shape selectivity) make these materials excellent candidates in heterogeneous catalysis.¹⁶⁶ Thus, a good MOF catalyst should have: i) functionalized organic ligands to activate the reactions, as for instance, in Brønsted acidity; ii) coordinatively unsaturated metal sites; and iii) the potential to incorporate metal complexes into the organic ligand and pores/channels.¹⁰ To enhance the catalytic performance of MOFs, researchers have employed two main strategies to date: i) postsynthetic modifications of the porous inner surface of MOFs,¹⁶⁷ or ii) the encapsulation of metal nanoparticles,¹⁶⁸ or other compounds (*e.g.*, polyoxometalates),¹⁶⁹ using the porous MOF structure as host matrices to support the catalysis.

MOFs have been playing decisive roles in various catalytic transformations, of which we emphasize:

- Aerobic oxidation of alcohols;¹⁷⁰
- C-C coupling reactions;¹⁷¹
- CO to CO₂ oxidation;¹⁷²
- Knoevenagel condensation reactions;¹⁷³
- Cyanosilylation of aldehydes;¹⁷⁴
- Asymmetric alkene epoxidation;¹⁷⁵
- Mukaiyamaaldol reactions;¹⁷⁶
- Hydrogenation of aromatic ketones;¹⁷⁷
- Oxidation of alcohols to ketones;¹⁷⁸
- Catalytic oxidative desulfurization;¹⁶⁹

- Ring-opening reaction of epoxides.¹⁷⁹

To demonstrate the importance of the organic linkers in heterogeneous catalytic studies Hasegawa *et al.* prepared the 1,3,5-benzenetricarboxylic acid tris[*N*-(4-pyridyl)amide] (4-btapa) ligand with three amide groups, which could act as guest interaction sites, and three pyridyl groups to coordinate to the metallic centres.¹⁷³ The self-assembly of 4-btapa with Cd²⁺ cations gave rise to a 3D porous network, formulated as {[Cd(4-btapa)₂(NO₃)₂]}_n·6H₂O·2DMF, with the amino groups ordered uniformly on the surface of the inner channels. This heterogeneous catalyst was used in the Knoevenagel condensation between benzaldehyde with active methylene compounds (*e.g.*, malononitrile, ethyl cyanoacetate and cyano-acetic acid *tert*-butyl ester). Results demonstrated that the selective heterogeneous base catalytic properties of the MOF (due to the active amino groups) depend on the size of the reactants: the malononitrile was a good substrate leading to 98% conversion of the adduct, while the remaining substrates reacted negligibly (Figure 12).

→ Insert Figure 12 ←

The highly porous UiO-66-CAT MOF can be obtained from both post-synthetic deprotection (PSD) and post-synthetic exchange (PSE) strategies.¹⁷⁸ The catechol units present in UiO-66-CAT coordinate to Fe and Cr through the use of Fe(ClO₄)₃ and K₂CrO₄ as starting chemicals, respectively, with the structure of the MOF being decorated with coordinatively and catalytically active metal sites. The catalytic performance of UiO-66-CrCAT was investigated in the oxidation reaction of a handful of secondary alcohols to the respective ketones, with results indicating that: i) catalytic reactions could be achieved with very low Cr loadings (0.5-1 mol %); ii) almost all desired ketones were obtained in very good to excellent yields in periods of time varying between 8 and 24 h; iii) UiO-66-CrCAT is a true heterogeneous catalyst; and iv) UiO-66-CrCAT could be reused over five catalytic runs without any significant loss in the catalytic activity.

Chen *et al.* reported for the first time the incorporation of bimetallic core-shell nanoparticles into the pores of a mesoporous MOF (Figure 13).¹⁸⁰ The Cr(III)-based MIL-101 (with giant pores ranging from 2.9 to 3.4 nm) was selected as a host matrix to incorporate the Pd@Co core-shell nanoparticles using ammonia borane (NH₃BH₃, AB) as the reducing agent (Figure 13). The resulting Pd@Co@MIL-101 catalyst, as well as Pd@Co/MIL-101 (material having the Pd@Co core-shell nanoparticles deposited on the external surface of MIL-101), were tested in the hydrolytic dehydrogenation of AB under mild conditions (30 °C at normal pressure). The initial catalytic activity of Pd@Co@MIL-101 slightly surpasses that of Pd@Co/MIL-101. Additionally, the recyclability of both catalysts was evaluated in five consecutive runs: while the catalytic activity of Pd@Co/MIL-101 in the reaction of generation of H₂ decreases considerably during the recycling experiments, the performance of Pd@Co@MIL-101 remains unaltered without the need of any treatment or activation. This behaviour is, probably, due to the nanoparticles incorporated and stabilized inside the pores.

→ Insert Figure 13 ←

Polyoxometalates (POMs) have exhibited high catalytic activity for aerobic oxidations. Song and collaborators explored this advantage by preparing POM-MOF composite materials. In 2011, this research group encapsulated the Keggin-type POM [CuPW₁₁O₃₉]⁵⁻, a good catalyst for air-based organic oxidations, into the well-known HKUST-1, ultimately isolating a novel POM-MOF [Cu₃(C₉H₃O₆)₂]₄[{(CH₃)₄N}₄CuPW₁₁O₃₉H]₄·40H₂O. This resulting material was tested in the aerobic H₂S oxidation in aqueous solutions and under gas phase (solvent-free), and also in the aerobic oxidation of thiol.¹⁸¹ The study revealed that the POM-MOF catalyst is highly robust, showing a mutual enhancement of stability originating from both the MOF and POM components. It was further observed that the POM-MOF catalyst is highly efficient in catalytic reactions of detoxification of several sulphur compounds including H₂S and S₈ using solely air: the toxic H₂S is rapidly removed *via* the H₂S + ½ O₂ → 1/8 S₈ + H₂O reaction.

2.2.5 - Luminescence

Luminescence is normally used to describe the process where light is produced by the emission of energy from a material,²¹ and contains two basic forms: i) fluorescence which is spin-allowed, possessing typical lifetimes ranging between nano- to microseconds; and ii) phosphorescence, being spin-forbidden, and having lifetimes which can reach several seconds.²² The possibility to simultaneously fine-tune the organic and inorganic components of a given material can permit the modification of the optical properties of the final materials. Light emission may appear either from individual organic ligands or metallic centres, or from materials resulting from their interconnection. Thus, the luminescent properties of a given MOF may arise from: i) organic ligand-based luminescence, including both the ligand-to-metal charge transfer (LMCT) and metal-to-ligand charge transfer (MLCT) phenomena; ii) adsorbate-based emission and sensitization, the so-called *antenna effect*; iii) surface functionalization; and iv) scintillation.²²

Luminescent MOFs have been over the years constructed from the self-assembly of very distinct organic linkers and metallic centres (lanthanides and transition metals). Some of them exhibit great potential to be applied as sensors to detect VOCs and explosive molecules,¹⁸²⁻¹⁸⁷ ions,¹⁸⁸⁻¹⁹¹ pH sensors,¹⁹² for bioimaging and intracellular sensing¹⁹⁰ and to produce luminescent nanothermometers to be used in nanotechnology and biomedicine.¹⁹³

In 2011 the research group led by Kitagawa reported a remarkable example of a luminescent MOF based on the porous $[\text{Zn}_2(\text{bdc})_2(\text{dpNDI})]_n$ framework prepared from a mixture composed of benzene-1,4-dicarboxylic acid (H_2bdc) and N,N' -di(4-pyridyl)-1,4,5,8-naphthalenediimide (dpNDI) organic linkers and $\text{Zn}(\text{NO}_3)_2$ in DMF, under solvothermal conditions.¹⁹⁴ Even though the new dpNDI linker predictably has a low fluorescence quantum yield, authors deduced that this molecule could strongly interact with aromatic VOCs. The obtained materials exhibited a strong colour change in the visible region of the spectrum, being this a direct consequence of the adsorbed aromatic VOC. The incorporation of benzene, toluene, xylene, anisole and iodobenzene into the porous framework of desolvated $[\text{Zn}_2(\text{bdc})_2(\text{dpNDI})]_n$, led to new products (*i.e.*, $[\text{Zn}_2(\text{bdc})_2(\text{dpNDI})]_n > \text{VOC}$) displaying intense blue, cyan, green, yellow, and red photoluminescence, respectively (Figure 14). This chemoresponse was of a non-linear nature owing to the coupling of structural transformation with the amount of adsorbed guest molecules.

→ Insert Figure 14 ←

More recently, Joarder *et al.* described the 3D bio-MOF-1, formulated as $[\text{Zn}_8(\text{ad})_4(\text{BPDC})_6\text{O}\cdot 2\text{Me}_2\text{NH}_2]\cdot \text{G}$ ($\text{G} = \text{DMF}$ and water molecules), for the detection of the nitroexplosive 2,4,6-trinitrophenol (TNP).¹⁸² Preliminary tests revealed that bio-MOF-1 immersed in water for several weeks retains its crystallinity, confirming its hydrolytic stability. The reported MOF also showed identical stability in TNP solution: the free amine groups located into the pores of bio-MOF-1 ensure an easy and strong interaction with the guest molecules. Taking advantage of the stability in water, the dehydrated form of bio-MOF-1 was evaluated in sensing essays using several nitroexplosives in aqueous medium (*i.e.*, TND, TNP, RDX, DMNB, NM, 2,4-DNT and 2,6-DNT). The emission response was monitored by fluorescence titration and, besides TNP, almost all the others nitroexplosive compounds induced quenching in the luminescent behaviour of bio-MOF-1. Additional studies revealed an unprecedented sensitive luminescence-quenching efficiency for TNP.

The microporous MOF-253, assembled from 2,2'-bipyridine-5,5'-dicarboxylic acid residues coordinated to Al^{3+} cations, was firstly reported by Bloch *et al.* in 2010.¹⁹⁵ Four years later, Yan's group isolated the same material at the nanoscale with the particle size ranging from *ca.* 50 to 300 nm by adding to the reaction mixtures acetic acid (HAc) or sodium acetate (NaAc):¹⁹⁰ i) MOF-253 (α) (addition of HAc); ii) MOF-253 (β) (without HAc and NaAc); and MOF-253 (γ). From transmission electronic microscopy (TEM) authors discovered that the length of the particles (with rectangular shape) varied according to the addition of HAc or NaAc: about 300 nm for MOF-253 (α), 150 nm for MOF-253 (β) and 50 nm for MOF-253 (γ). This variation induces modifications in the full-width-at-half-maximum (FWHM) of the powder X-ray diffraction patterns, being larger for MOF-253 (γ) (material with smaller particles). The Langmuir surface areas have also different values due to the particle size, being of *ca.* 1092, 1183 and 1272 $\text{m}^2 \text{g}^{-1}$ for MOF-253 (α), MOF-253 (β) and MOF-253 (γ), respectively. The

dehydrated phase of the smaller MOF-253 (γ) was used for the detection of different metal cations (*i.e.*, Na^+ , Mg^{2+} , Ca^{2+} , Fe^{2+} , Co^{2+} , Ni^{2+} , Cu^{2+} , Zn^{2+} , Pd^{2+} , Cd^{2+} , Ba^{2+} , Cr^{3+} and Fe^{3+}) in aqueous solutions. From fluorescence studies, it was found that only Fe^{2+} induces a substantial quenching on the fluorescence of MOF-253 (γ), suggesting a high selectivity of this material towards the recognition of Fe^{2+} in aqueous solutions (Figure 15 - *left*). The cytotoxicity of MOF-253 (γ) was further investigated by introducing this material into HeLa cells. After incubation with different concentrations of MOF-253 (γ) (10, 15, 20, 25, 30 and 35 $\mu\text{g mL}^{-1}$) for 24 h, more than 85% of the HeLa cells remained alive, with the results revealing that this nano-sized MOF material exhibits low toxicity towards cell proliferation. Figure 15 (*right*) depicts the confocal fluorescence ($\lambda_{\text{ex}} = 405 \text{ nm}$) and brightfield images of the HeLa cells incubated with 5 μM of MOF-253 (γ) for 3 h at 37 $^{\circ}\text{C}$.

→ Insert Figure 15 ←

A MIL-type MOF formulated as $[\text{In}(\text{OH})(\text{bpydc})]$ (where $\text{H}_2\text{bpydc} = 2,2'$ -bipyridine-5,5'-dicarboxylic acid, the same organic ligand used to isolate MOF-253), was prepared by Zhou *et al.* in the nanoscale range (particle sizes varying between *ca.* 40 and 140 nm).¹⁹³ Aiming at post-synthetic functionalization, the obtained MOF was soaked in DMF with lanthanide(III) chloride salts: i) Eu^{3+} , ii) Tb^{3+} and iii) a mixture of $\text{Eu}^{3+}/\text{Tb}^{3+}$ (0.005/0.995). This post-synthetic procedure allowed the incorporation of lanthanide cations into the structure of $[\text{In}(\text{OH})(\text{bpydc})]$, giving rise to $\text{Eu}^{3+}@[\text{In}(\text{OH})(\text{bpydc})]$, $\text{Tb}^{3+}@[\text{In}(\text{OH})(\text{bpydc})]$ and $\text{Eu}^{3+}/\text{Tb}^{3+}@[\text{In}(\text{OH})(\text{bpydc})]$ materials isotypical with the parent material. To evaluate the performance of the lanthanide@ $[\text{In}(\text{OH})(\text{bpydc})]$ MOFs in temperature sensing, the temperature-dependent luminescent spectra and the lifetimes of the three materials were measured. Results showed that, on the one hand, the emission intensity and decay time of Tb^{3+} in $\text{Tb}^{3+}@[\text{In}(\text{OH})(\text{bpydc})]$ decreased abruptly with the increasing temperature; on the other hand, the luminescence and lifetime of Eu^{3+} in $\text{Eu}^{3+}@[\text{In}(\text{OH})(\text{bpydc})]$ did not suffer significant modifications, clearly showing that this particular material was not sensitive to temperature. The temperature-dependent luminescent behaviour of Eu^{3+} and Tb^{3+} in the mixed-metal $\text{Eu}^{3+}/\text{Tb}^{3+}@[\text{In}(\text{OH})(\text{bpydc})]$ material is, however, strikingly different. While increasing the temperature from *ca.* 10 to 60 $^{\circ}\text{C}$ one observes that the Tb^{3+} emission decreases more than *ca.* 60% when compared with the *ca.* 33% observed for Tb^{3+} in $\text{Tb}^{3+}@[\text{In}(\text{OH})(\text{bpydc})]$. Additionally, the Eu^{3+} emission in $\text{Eu}^{3+}/\text{Tb}^{3+}@[\text{In}(\text{OH})(\text{bpydc})]$ increases, being the exact opposite of that observed in $\text{Eu}^{3+}@[\text{In}(\text{OH})(\text{bpydc})]$. The registered variations at different temperatures of Eu^{3+} and Tb^{3+} emissions in the $\text{Eu}^{3+}/\text{Tb}^{3+}@[\text{In}(\text{OH})(\text{bpydc})]$ demonstrate the possibility of this MOF material to be applied as a nano-platform for temperature sensing, clearly evidencing at the same time that the properties of the mixed-lanthanide compound are much more than the simple sum of those observed for the individual materials.

2.2.6 – Metal corrosion inhibition

Corrosion of metal surfaces is a natural process induced by environmental conditions. Tackling this phenomenon (if possible through the implementation of a “green” approach) can be, however, highly expensive. Everyday metallic-based materials (containing as, for instance, iron, steel, copper, zinc, among others) suffer corrosion owing the exposure to oxygen or other oxidizing agents (*e.g.*, H_2O_2 and BO_3^-). Therefore, the development of metal corrosion inhibitors is currently an active research field of great industrial interest in order to clean/remove the oxide layer of the metallic surfaces, which leads to severe corrosion and metal loss. Several anti-corrosion agents have been reported in the literature and MOF compounds emerge as potential candidates.^{73, 75, 196-199} This family of materials, typically with high surface areas, wide supramolecular natures and unique topologies, being rich in π -systems and heteroaromatic moieties, should thus attract the interest of industry and society while being employed as corrosion inhibitors.¹⁹⁸

Demadis's research group pioneered the preparation of organic-inorganic hybrid networks with inhibiting effect on metallic corrosion.²⁰⁰ These authors reported multidimensional MOFs from the self-assembly of phosphonate- or sulfonate-based organic linkers and alkaline, alkaline-earth and transition metal centers.^{75, 196-197, 200-201} In 2008, they reported a series of layered or three-dimensional coordination

polymers, generally coined as M-HPAA [where HPAA = hydroxyphosphonoacetate; and M = Ma, Ca, Sr and Ba], obtained from hydrothermal synthesis from the adjustment of the pH of the reactive mixtures to 2.7 using NaOH.⁷⁵ The resulting M-HPAA materials were formulated as $\{M[(HPAA)(H_2O)_x] \cdot (H_2O)_y\}_n$ with x and y determining the amount of metal-coordinated and lattice water. Corrosion inhibition experiments involved the exposure of carbon steel specimens in synergistic combinations of M^{2+} (Sr^{2+} or Ba^{2+}) and HPAA in oxygenated aqueous solutions, with a M:HPAA molar ratio of 1:1 while varying the pH (2.0 and 7.3). Results suggest that when Sr-HPAA and Ba-HPAA materials are generated *in situ* at pH 2.0, in an aqueous solution in contact with a carbon steel specimen, both compounds are unable to avoid metallic corrosion, being the corrosion rates dramatically higher than the “control” (Figure 16). On the other hand, at pH 7.3 both Sr-HPAA and Ba-HPAA act as effective corrosion inhibitors (with an inhibition efficiency of approximately *ca.* 100%) generating anticorrosion protective films on the carbon steel surface (Figure 16).

Etaiw and co-workers described the synthesis of a new MOF, $[(AgCN)_4 \cdot (qox)_2]$, by combining Ag^+ cations with the quinoxaline organic ligand.¹⁹⁸ The MOF was employed as corrosion inhibitor for carbon steel surfaces. Typical polarization curves of carbon steel in an aqueous solution of HCl (1 M) in the presence or absence of the hybrid material were collected with results indicating that the $[(AgCN)_4 \cdot (qox)_2]$ MOF is an effective corrosion inhibitor for carbon steel.

Although copper surfaces are more resistant to reactive environments when compared with other metallic ones, this element is also susceptible to corrosion. Fernando *et al.* investigated the capacity of some layered inorganic-organic networks as corrosion inhibitors of copper surfaces.¹⁹⁶ MOF structures were prepared by reacting the organic ligand pyrazole-4-sulphonic acid (4-SO₃-pzH) with ZnO, CdCO₃ and Ag₂O, with the resulting materials being formulated as $[Zn(4-SO_3-pzH)_2(H_2O)_2]$, $[Cd(4-SO_3-pzH)_2(H_2O)_2]$ and $[Ag(4-SO_3-pzH)]$. These compounds, as well as the organic linker, were studied in corrosion studies performed at three different pH values (2.0, 3.0 and 4.0). Results demonstrated that the copper surfaces were satisfactorily protected with all compounds, mainly at pH 3 and 4.

→ Insert Figure 16 ←

3 - MOF production at the industrial scale

In the previous sections we have highlighted some striking functional MOFs which, by their properties, could arise as potential materials for applications in industry and in our daily life. In the following sections we shall direct our attention to what has been made in the last years to make this academia-to-industry transposition a reality, namely in the form of patents by industry and the production in large scale of MOFs typically used in a wide variety of applications.

3.1 - Financial and environmental viability

As mentioned in the beginning of the present review, MOFs can be prepared in the laboratory using a myriad of methods. Nonetheless, some of them seem to be more industrially feasible than others. Bringing back the well sedimented knowledge on zeolite chemistry, in particular its large-scale production, solvothermal synthetic routes arise as the most feasible for industrial transposition.²⁰² To perform reactions under solvothermal conditions the metal centres are typically sourced from inorganic salts, the organic ligands selected among those industrially available, and polar organic solvents preferentially chosen. The straightforward selection of the raw materials greatly impacts the large-scale implementation because the price per Kg of the final MOF has to be as low as possible. Müller published an excellent industrial outlook on MOFs summarizing very well this point: oxides and sulphates are preferentially chosen as metals centres, and carboxylic acids chosen (*e.g.*, terephthalic, isophthalic and formic acids) as the basis of the organic linkers instead of those more complex and not readily available.²⁰² Müller further considered the Space-Time-Yield of synthesis (STY, Kg of MOF product per m³ of reaction mixture per day of synthesis).^{26, 202} This parameter is of great interest when planning large scale implementation and it should be as high as possible to make sure the reaction is financially attractive. STY has a close relation with the costs of the chosen raw materials (in particular those of the

linker and the solvent), and of the reaction vessel needed to perform the reaction. Intrinsic high costs have to do with the requirement of pressure-sealed vessels and heating machinery under high and controlled temperature working during several days. Additionally, major investments may be required to handle the low chemical resistance of a certain reactor, or to cope with diluted processes that may need large quantities of solvents or bulky reactors to obtain the desired quantity of product within the same time frame (Figure 17).

→ Insert Figure 17 ←

Post-reaction costs strongly influence the financial attractiveness: filtration, washing and drying procedures cannot be time and cost expensive, given the amount of solvent needed and the duration of the processes (including waste disposal). Noteworthy, such post-reaction steps are significantly influenced by the agitation during chemical reaction: if the latter parameter does not promote homogeneous reacting conditions (in terms of dispersion of the reactants and heat transfer), technical concerns will arise when collecting the final product, in particular those related to physical and chemical properties, not to mention the possibility of formation of secondary products. Among other parameters, one has to guarantee the production of a MOF with the proper crystallite size, morphology, porosity, surface area and purity in order to fulfil its final applications.

Though we have pointed the drawbacks limiting the scale-up production of MOFs by means of solvothermal procedures, we also have to account for the environmental sustainability (by decrease or avoidance of toxic by-products releasing), the energy consumption and safety issues during reaction (either related to the autogenous pressures observed or to the hazard of reactants and solvents used).^{3, 7} It is, thus, clear that this is not an easy task, and many reported MOFs in the literature suffer from many limitations when concerning their possible industrial transposition.

3.2 - Market Opportunities and Commercial applications

A wide range of promising functional MOFs have been reported to date, and their potential use in several technological fields investigated in detail (see our selection of promising areas and materials in the previous subsections). However, only very recently applications ceased to be a purely academic idea to find their way into reality and daily life.²⁰³ Mainly driven by the quest for porosity and large surface areas, MOFs are thus today promising materials for gas storage, uptake and separation, as well as good candidates to perform heterogeneous catalytic reactions. It was, thus, a matter of time until the full development of industrial scale-up processes for some remarkable MOF compounds. In this context, the company BASF claims to have been the pioneer in the large-scale production of MOFs through the development of an electrochemical method for the industrial preparation of HKUST-1 (US8163949B2 patent).^{9, 26, 204}

3.2.1 - Examples on large-scale production of MOFs

Chemical companies like BASF and MOF Technologies have been improving the manufacturing techniques of MOFs aiming at bridging the academic knowledge on their synthesis to the needs of their sustainable production by the tonne. BASF was the first industrial company showing interest in MOFs and, therefore, the first to successfully achieve a large-scale production. They early foresaw the technological importance that these materials could represent, mainly because of their outstanding surface areas and their possibility to be synthesized with readily available and cheap reactants. For the past decade, BASF focused on basic research and developed an interesting portfolio of MOFs (sold under the tradename Basolite™, Table).

→ Insert Table 2 ←

BASF's key role in MOFs affirmation was recognized in the form of a prize, the French Pierre Potier Prize, attributed in 2012 by the two French chemical associations emphasizing the chemical

research pointing towards the sustainable development and green chemistry of MOFs. A remarkable breakthrough by BASF was accomplished when the solvothermal preparation of Basolite A520 was fully optimized into a hydrothermal synthesis for industrial implementation (by the tonne).²¹³

The compounds commercialized by BASF are currently being sold by Sigma-Aldrich and, thus, available as raw materials to the entire community. Nevertheless, other companies compete to expand or improve this portfolio of MOF raw materials:

(i) MOF Technologies patented a technology based on mechanochemistry, allowing the large-scale synthesis of several MOFs using small amounts (or even the absence) of solvents while also greatly reducing the preparation timescale. Striking examples are MTA1 (Al-based MOF), MTA2 (ZIF-8), MTA3 (ZIF-67) and MTA4 (HKUST-1);

(ii) Strem Chemicals supply ZIF-8. Their main breakthrough relies, however, on the commercialization of KRICT F100 (a fluorine-free version of MIL-100(Fe) prepared under hydrothermal conditions; US8507399B2 patent),²¹⁴ and UiO-66 (a Zr-based MOF with very high surface area and unprecedented thermal, chemical and mechanical stability; US20120115961A1 patent).²¹⁵

3.2.2 - Industrial Property

The continuous report of new crystalline structures is no longer a priority. Focus is instead on the preparation of (multi)functional materials able to solve a certain problem or to outperform other existing materials in a given task. The final goal would be, in any case, a market implementation. In this context, the more prolific is research on MOFs, the greater is the number of filed patent requests. A quick search on the European Patent Office database, relating to worldwide industrial property on MOFs reveals more than a thousand patents reported to date.²¹⁶ Claims cover a wide range of ideas from new MOF compounds, new preparation methods, to applications or improvements thereof.

Considering that industrial companies have been much more involved in MOF research (Figure 18), the increasing number of patents is a clear step forward to their commercial application. The way scientists look to MOFs has certainly changed since the seminal patent US5648508A,²¹⁷ “Crystalline metal-organic microporous materials for purification of liquids and gases”, assigned to NALCO Chemical Company and Omar Yaghi in 1995. Figure 18 highlights some recent trends on patent publications. Noteworthy, there is a significant increase of the number of patents filed by North American companies, a clear evidence of their growing interest on such compounds. Also remarkable is the fact that most part of German patents has been filed by BASF, proving the strong commitment and willingness of this company to use MOFs in the near future. It could be interesting to evaluate if the published patents concerning new MOF materials or methods to prepare them supplant those related to their final applications. However, this kind of examination would be arduous and tedious, and it would be difficult to draw conclusions given that many patents overlap different types of claims.

→ Insert Figure 18 ←

In the following subsection we emphasize some recent remarkable examples on the will to bring MOF academic knowledge to the industrial implementation.

3.2.3 - Transport and Oleochemical industry

Transport arises as the technological field in which MOF industrial applications are more developed, with most of the efforts dealing with innovative solutions for fuel storage, separation and catalysis. The typical high surface areas of MOFs, allied with their high selectivity and favourable energetics for adsorbing gas (see examples in previous subsections), made possible projects like EcoFuel Asia Tour (in 2007): a journey through 14 countries in a car (Volkswagen Caddy EcoFuel) which was optimized for natural gas combustion and using MOF-enhanced fuel tanks (sponsored by BASF; Figure 19). The choice for Basolite C300 (HKUST-1) was based on previous knowledge relating to its high storage capacity for natural gas. Pellets of this MOF were placed inside a traditional tank, which was later

filled with CNG (compressed natural gas). It was reported a boost in storage capacity of about 30% compared with the empty tank, and an increase of about 20% in the distance the car could travel without refuelling. Moreover, overall statistics relating to the whole tour pointed for an average consumption of 7 Kg of natural gas per 100 km and 1.3 tons less of CO₂ emissions (when compared to a Volkswagen Caddy 1.6 L petrol engine).^{202, 218} Road tests on CNG vehicles (passenger cars and large trucks)²¹⁹ have been under consideration since 2007, and BASF has already, at least, two registered prototypes for gas storage (BASOCUBE™ and BASOSTOR™), which have also been studied for hydrogen storage. Compared to CNG, hydrogen usage raises more safety issues because of its less dense nature and requirement for better seals.²⁰² Nevertheless, BASF was able again to prove that MOFs can enhance hydrogen storage performance with Basolite Z377 (MOF-177). When using this compound in a 50-L prototype container, it was possible to fill the tank within 5 min at 50 bar and 77 K, and to obtain volume-specific capacities of 23 and 37 g(H₂)L⁻¹ for gaseous hydrogen at 350 bar/298 K and 700 bar/298 K, and 71 g(H₂)L⁻¹ for liquid hydrogen at 1 bar/20 K, respectively.^{202, 212} Ford Motor Company (in collaboration with BASF), when performing round-robin validation measurements on hydrogen uptake by five different Basolite™ compounds (Z377, Z100-H, Z200, Z1200 and M050), also followed the aforementioned tendency with maximum uptake values at around 7 wt% H₂ for the same compound, and 8 wt% H₂ for Basolite Z100-H (MOF-5).

→ Insert Figure 19 ←

The interest on moving MOFS towards commercial applications is clearly proven by two recent patents filed by Ford Global Technologies (a subsidiary of Ford Motor Co. owing, managing and commercializing its patents and copyrights) named as: “Hydrogen Storage Materials” (US20110142752A1)²²⁰ and “Hydrogen Storage Systems and Method using the same” (US20110142750A1).²²¹ Another striking example on hydrogen storage concerns the zero-emission Mercedes-Benz F125® (research) vehicle using hydrogen stored in MOFs.²²² In all instances, the industrial implementation has been delayed due to technical barriers such as system weight, volume, cost, efficiency and durability.

Ford Motor Co. also invented an electrochemical battery system for use in vehicles, comprising a metal oxygen battery containing oxygen storage materials, among which some are MOFs (US8658319B2).²²³ Oxygen is contained by physisorption intercalation and/or clathratization in relatively high concentrations. This method also describes an increased efficacy and reduction of system costs because it avoids the presence of interfering gas molecules, such as nitrogen. The operating approach allows different electrode configurations (*e.g.*, planar cell or jelly roll) and it is based on reversible redox reactions in which the oxygen is released during a discharging reaction and stored during the charging stage.

Another striking example on MOF-based batteries comes from Toyota which has recently filed a patent for a magnesium ion battery comprising a cathode having an active material based on a MOF framework, and an anode composed of a non-aqueous electrolyte containing magnesium ions (US patent application 20150044553).²²⁴

Current industrial examples involve other companies such as Total Refining and Petrochemicals, interested in gas separation and storage, liquid separation and catalysis. For instance, invention WO2014009611A1 describes the use of MOFs in a cyclic method for the separation of high purity nitrogen (> 95 mol%) and a hydrocarbon from a mixture of both compounds.²²⁵ Architectures such as MIL-100(Fe), MIL-125(Ti), MIL-125(Ti)-NH₂, HKUST-1 or UiO66 have been used to boost the separation performance using the least possible energy. WO2012089716A1 and WO2012004328A1 patents deal with the preparation of nitrogen-depleted hydrocarbon feedstocks for the refinery industry.²²⁶⁻²²⁷ MOFs are used as nitrogen adsorbents in the purification step of a process of hydrocarbon feedstock molecular weight increase *via* olefin oligomerization and/or olefin alkylation onto aromatic moieties.

ENI (oil and gas company) and Haldor Topsoe (catalysis and surface science), have recently participated in an academy-industry consortium dedicated to the study of heterogeneous catalysts based on two different families: CPO-27-M (where M = Ni, Mg, Co, Mn) and Zr based UiO-66 (an isorecticular family comprising three compounds with increasing length of the linker). Results showed significant

amounts of stored hydrogen for both families, and a particular high methane storage for the case of CPO-27-Ni.²²⁸ Novel MOFs for hydrodesulphurisation of oil were prepared and tested for their catalytic performance, demonstrating nearly twice the activity of the commercial competitor, the high-surface area alumina-supported CoMo catalyst.²²⁸

Examples on industrial research also include the Johnson Matthey company in the same topic of catalysis and materials science.²²⁹ Two patents have been recently filed by this company concerning a compound and its preparation method (WO2013160683A1, filed in 2013),²³⁰ and another method of MOFs manufacture resulting in high surface area materials (WO2014114948A1, filed in 2014).²³¹⁻²⁴⁰

It is important to emphasize that the thermal stability of MOFs is usually limited to temperatures below 400 °C, which somehow reduces their potential with respect to applications at high temperatures. Both thermal and chemical stability and efficiency/cost ratio are crucial when studying MOFs for catalytic purposes. These can be some of the main reasons why, over so many years of intense research, catalysts based on MOFs have yet not transposed the academic realm. Nonetheless, their remarkable strength relies in their ability to tailor the final structure to customer requirements, unveiling a possible tonne scale preparation and commercial breakthrough in the very near future.

3.2.4 - Textile industry

Textile technology is probably, and surprisingly for some, the second field on the edge of a commercial breakthrough using MOFs. These materials have been engineered according to pore size and functionalization in order to design protective clothing for chemical, biological, radiological and nuclear warfare (CBRN). These threats call for the best solutions of filtering personal protective equipment (for military, civil defence, law enforcement, first responder). Therefore, target industrial market segments include filtration garments capable of trapping harmful agents (aerosol, liquid and vapour forms), and to reduce the trauma risk, with extended life expectancy and the highest comfort. Materials are, thus, designed to obtain thin adsorbents, with suitable particle size for the chosen toxic agents, capable of high particle loadings, wash resistance, high air permeability and thermal and mechanical stability.

Ouvry company claims its SARATOGA[®] technology is currently the most trusted family of adsorptive compounds dedicated to CBRN protection in the world (with more than 150 filter material references). This commercial achievement is, however, based on spherical activated carbon adsorbents. Ouvry is currently dedicated to research and development of nanoscale MOF materials and their combination with air permeable textiles to design novel filters. A major asset of MOFs over other filtration systems is their high diversity of architectures (given the almost endless number of combinations of metals and organic ligands/functional groups), typically characterized by ordered and porous structures. In addition, examples on MOFs with resistance to humidity, rough handling (mechanical stability) and temperature (both in use or stored) makes these compounds suitable for devices with no significant decrease over time in efficiency and dust release.²⁴¹ For such reasons, MOFs guarantee an adsorption of almost all chemical vapour agents.

Besides Ouvry, joint (large-scale) efforts have also been undertaken by companies such as Norafin and Blücher. For instance, Norafin (in collaboration with Dresden Technical University) developed nonwoven materials from different fibres (such as PET, aramides, viscose and natural flax), which were coated with a polymeric binder (*e.g.*, acrylate, latex, ethylene vinylacetate and aliphatic polyester-polyurethane) to fix MOF particles at the fibre surface.²⁴² Immobilization of MOF particles was performed via electrospinning or direct chemical fixation, through MOF synthesis on the fibre surface or its simple entrapment in the void spaces within the fibres (Figures 20 and 21). Promising results using HKUST-1 and FeBTC have shown good performance for H₂S, NH₃ and cyclohexane retention. On the other hand, Blücher has also developed protective gloves from textile filters based on HKUST-1. Although the performance of MOFs in the presence of cyclohexane could be compromised under humid conditions, Blücher improved the adsorption ability of the textile filters by combining the MOF with conventional carbon based adsorbents.

→ Insert Figure 20 ←

→ Insert Figure 21 ←

Pioneering examples on large scale samples of textiles impregnated with MOFs have shown a remarkable performance. It is thus not surprising the emergence of patents related to processing of MOFs for textiles (e.g., WO2012156436A1, DE102009042643A1, and US20120237697A1).²⁴³⁻²⁴⁵

3.2.5 - Respiratory systems

Materials for respiratory purposes rely strongly on adsorptive capacities (such as those described previously for energy-based gases). Concerns and priorities are, however, rather different when compared to other applications based on the same physical principles. Considering the proximity of the final device to the person's respiratory tract and eyes, one has to achieve practical solutions with high performance under humid conditions (*ca.* 70% of relative humidity), high mechanical stability (either for their production or avoidance of arising of harmful wear residues), and low respiratory resistance.²⁴¹ Currently, gas mask filters are based on active carbon compounds that tune their adsorption selectivity by their impregnation with additives such as zinc, silver, copper, molybdenum and triethylenediamine. These systems are, however, typically based on weak physical adsorption interactions. In this context, MOFs emerge as promising alternatives given their ability to tightly sequester test agents (through, for example, covalent bonds).

Blücher is again a leading company on the research related to this topic, with recent efforts being devoted to the creation of filter canisters for personal protection (Figure 22).²⁴⁶ HKUST-1 was used as test material for cyclohexane, NH₃ and H₂S resistance, standing alone or combined with Polymer-based Spherical Activated Carbons (PBSAC). Blücher tested HKUST-1-PBSAC co-agglomerates, HKUST-1-PBSAC agglomerates, flat filter media with HKUST-1 and flat filter media with HKUST-1-PBSAC. Results have shown that both agglomerates and flat filters accomplish the demand for high adsorption capacity, low pressure drop and high mechanical stability. A filter solely based on HKUST-1 lags, however, behind in terms of pressure drop, which means that it could be only used as an additional layer (*i.e.*, supplementary filter) in the preparation of a filter canister. However, the combination of HKUST-1 with PBSAC proved to be beneficial. As an industrial demonstrator, Blücher used two different approaches: (i) a stack of nonwoven filters with the MOF and flat filter media with impregnated PBSAC; (ii) a stack of flat filter media with HKUST-1-PBSAC. Both stacks showed a breakthrough time above 60 min for all the tested gases, which is significantly high above the European directive EN14387 requirements for gas filters and combined filters (> 35 min for cyclohexane; > 40 min for NH₃ and H₂S). In addition, the required respiratory resistance was also fulfilled.

→ Insert Figure 22 ←

Besides the previously mentioned gases, respiratory protection masks might also deal with other toxic industrial chemicals (such as carbon monoxide or phosphorous gases) or chemical weapons (military protection).²⁴⁷ An example on the latter topic is the capture of nerve agents and mustard gas analogues by hydrophobic robust MOF-5 type compounds.¹⁵² To prove the real military interest on MOFs, please refer to the patent 8883676, filed in 2013 by the Secretary of the Army of USA: it describes the removal of toxic chemicals (ammonia, and cyanogens chloride – an asphyxiant that can be rapidly fatal) using MOFs (HKUST-1, MOF-177 or IRMOF compounds) post-treated *via* plasma-enhanced chemical vapour deposition with fluorocarbons.²⁴⁸

It must be emphasized that the same technology may be applied to prepare advanced filter systems for selective adsorption related to industrial feed and exhaust gases. Such applications would certainly have a significant environmental and economic impact.

3.2.6 - Food packaging

This technology field is, once again, based on adsorptive properties. It might be, however, a bit behind the previous examples when considering industrial implementation. One of the reasons is related with the potential (and poorly understood) side effects related to the use of MOFs in close contact with

food, being a direct consequence of the lack of studies reported in the literature concerning MOF toxicity. Nonetheless, two patented solutions try to overcome such limitations.

Mastertaste Inc. (ingredients and flavours company, and through inventors Herman Stephen and James Stuart) assigned a MOF-based system for odour sequestration and fragrance delivery (patent WO2007035596A2, filed in 2006).²⁴⁹ Malodours are low molecular weight volatile organic compounds (VOCs), commonly associated to dangerous or unhealthy situations (such as the presence of rotten food). The malodour control is often done by means of smell masking with high doses of fragrances based on a large variety of chemicals (such as zeolites, cyclodextrins or active charcoal, among many others). Researchers described their invention as a reliable platform to address every malodour situation: malodour molecule contacting with a MOF comprising a myriad of metals and linkers allows its control or elimination, even when in the presence of customized molecules; as well as the same MOF architectures allows the incorporation of fragrance compositions to be delivered afterwards.

The second example is the patent filed in 2010 by BASF (US20120016066A1),²⁵⁰ in which Ulrich Müller and co-workers describe a biodegradable material composed of a polymer comprising a porous MOF (in a proportion ranging between 0.01-10% by weight of the polymer). The patent relates to a material prepared as a foil or a film to be used afterwards for the adsorption of ethene in food packaging. It is well known that ethene can accelerate the ripening of foods such as fruits and vegetables. For that reason, several adsorbents have been used to remove this gas from food packages (*e.g.*, zeolites, silicas or activated carbons). The present solution from BASF can clearly compete with such compounds, for the proposed task, due to its increased versatility.

4 - Final Remarks

The strength of MOFs over other compounds strongly relies in their robust and well-defined structures, having linking units which are amenable to chemical modification by design.²⁵¹ They allow the establishment of different relationships between such structures and their final properties, then forecasting a wide range of potential applications.⁷ Unfortunately, during the first two decades of intense research on MOF materials, the final products were confined to a laboratory scale and no significant efforts were known for industrial implementation. The final result was a remarkably small percentage of truly functional MOFs that could be used in materials science and devices. Nevertheless, during the first two decades of MOF's intense research, a great wealth of valuable knowledge was gathered, as well as important experimental tools were acquired in worldwide leading laboratories.

This review highlighted striking compounds with outstanding potential for their application in several technological fields. Nevertheless, one should have caution regarding the likelihood of their general real-life implementation because of a number of important concerns. For the particular case of hydrogen storage, Müller has described those issues very well.²⁰² One of the main limitations arise with the need to cool down the hydrogen tanks (which does not happen for the equivalent gasoline-based systems), even when using a MOF as the filler. The second issue relates to the way the fuel is pumped: compressed or liquid. On the one hand, the high pressures associated to the compression of hydrogen demands better seals which implies an increase in the cost of production as well as a considerable safety risk. On the other hand, liquid hydrogen also requires special handling and the use of specific and expensive materials (not just inside the tank but everything around), because we must ensure the coldness of the fuel.²⁰² Even when MOFs are considered as promising alternatives to achieve ambitious storage targets and good candidates to mitigate (high pressure/low temperature) hydrogen storage conditions, one has to take into account that their industrial and commercial implementation could be expensive and difficult to achieve. The high cost of producing MOFs, associated in many cases with the use of expensive elements such as palladium,⁹⁶ might also hinder their industrial breakthrough. Note that this problem is also pertinent in other cases as, for instance, when using MOFs for packaging or most porosity-based applications. Beyond that, chemical stability and synthetic reproducibility are also desired and seek, because high purity compounds have been pointed as detrimental to achieve promising results in hydrogen storage capacities.²⁵²

Many of the aforementioned concerns related to hydrogen storage also arise when dealing with methane or natural gas. For the latter case, gas contamination and disintegration should also be taken into

account. This energy source has been used to fill MOF-enhanced tanks and it was observed the appearance of a small amount of sulfur contamination and the formation of a considerable quantity of fine particles in the tank. While the former case could be justified by sulfur-based odorants present in the natural gas, the second was attributed to the attrition experienced by the MOF particles during operation (rough handling).²⁰² Indeed, mechanical issues (*e.g.*, stability and phase integrity) related to the use of MOFs have been largely unexplored in the literature. Typically, these compounds are obtained as loose powders (composed by small crystallites) with low packing densities.^{202, 253-254} For that reason, they have to be shaped into suitable geometries (granules, extrudates or monoliths), in order to resist attrition and avoid disintegration into powders that could contaminate tanks, pipes or other apparatus.²⁵³⁻²⁵⁴

Fortunately, and as clearly shown in the present review, many novel functional MOFs have broken the laboratory boundaries and evolved in the past half-decade. We still do not know for sure if MOFs can compete with today's well-known industrial compounds (as zeolites, silicas or active carbons), but we are rather close to answer this question. As several worldwide researchers have been defending by means of focusing their work on MOF applications, it is time for these compounds to prove how they can benefit society both in fundamental and technological problems. It is time to MOF-based researchers to prove that MOF materials are vital to our modern lifestyle and, therefore, can establish their technological and industrial importance. This change of mind has already started with a large number of patents filed to date and also some interesting direct applications found as commercial products. Future challenges involve the preparation of MOFs as well as MOF-based devices in a simple, easy, green and low-cost way and in large amounts capable to cover the required necessities.

5 – List of Abbreviations

2,4-DNT	2,4-Dinitrotoluene
2,6-DNT	2,6-Dinitrotoluene
3D	Three-dimensional
BCES	Bis(2-chloroethyl)sulfide
BDC	1,4-Benzenedicarboxylic acid
BDP	1,4-Bis(pyrazol-4-yl)benzene
BET	Brunauer, Emmett and Teller
BPDC	Biphenyl dicarboxylic acid
bpy	4,4'-Bipyridine
bpydc	2,2'-Bipyridine-5,5'-dicarboxylic acid
BT	Benzothiophene
btapa	1,3,5-Benzenetricarboxylic acid tris[<i>N</i> -(4-pyridyl)amide]
BTC	1,3,5-Benzenetricarboxylic acid
CBRN	Chemical, biological, radiological and nuclear
CNG	Compressed natural gas
CP	Coordination Polymer
DES	Diethylsulfide
DIFP	Diisopropylfluorophosphonate
DMF	<i>N,N'</i> -dimethylformamide
DMNB	2,3-Dimethyl-2,3-dinitrobutane
DOE	Department of Energy
dpNDI	<i>N,N'</i> -di(4-pyridyl)-1,4,5,8-naphthalenediimide
FIB-SEM	Focused ion beam scanning electron microscopy
FWHM	Full-width-at-half-maximum
GO	Graphite oxide
HKUST	Hong Kong University of Science and Technology
HPAA	Hydroxyphosphonoacetate
IMFP	Isopropylmethylfluorophosphate
IND	Indole
IRMOF	Isorecticular Metal-Organic Framework

LMCT	Ligand-to-metal charge transfer
MIL	Materials Institute Lavoisier
MLCT	Metal-to-ligand charge transfer
MMM	Mixed matrix membrane
MOF	Metal-Organic Framework
NCC	Nitrogen-containing compound
NM	Nitromethane
NMR	Nuclear Magnetic Resonance
NOTT	Nottingham
NU	Northwestern University
PBSAC	Polymer-based Spherical Activated Carbons
PBU	Primary Building Unit
PCN	Porous Coordination Network
POM	Polyoxometalate
PPCP	Pharmaceutical and personal care product
PSD	Post-synthetic deprotection
PSE	Post-synthetic exchange
qox	Quinoxaline
QUI	Quinolone
RDX	1,3,5-Trinitro-1,3,5-triazacyclohexane
SCC	Sulphur-containing compound
SNU	Seoul National University
4-SO ₃ -pzH	Pyrazole-4-sulphonic acid)
STP	Standard temperature and pressure
STY	Space-time-yield
TEM	Transmission electronic microscopy
THF	Tetrahydrofuran
TNP	2,4,6-Trinitrophenol
TNT	2,4,6-Trinitrotoluene
UiO	Universitetet i Oslo
UMCM	University of Michigan Crystalline Material
UTSA	University of Texas at San Antonio
VOC	Volatile Organic Compound
ZIF	Zeolitic Imidazolate Framework

6 - Acknowledgements

We are grateful to *Fundação para a Ciência e a Tecnologia* (FCT, Portugal), the European Union, QREN, FEDER under the PT2020 partnership agreement, associated laboratory CICECO – Aveiro Institute of Materials (Ref. FCT UID/CTM/50011/2013) and QOPNA research unit (Pest-C/QUI/UI0062/2013) for their general funding scheme. We further wish to thank FCT for funding the R&D FCOMP-01-0124-FEDER-041282 (Ref. FCT EXPL/CTM/-NAN/0013/2013) and for the postdoctoral research scholarship No. SFRH/BPD/94381/2013 (to SMFV).

7 - References

1. S. R. Batten, N. R. Champness, X.-M. Chen, J. Garcia-Martinez, S. Kitagawa, L. Öhrström, M. O'Keeffe, M. P. Suh and J. Reedijk, *Crystengcomm*, 2012, **14**, 3001-3004.
2. D. J. Tranchemontagne, J. L. Mendoza-Cortés, M. O'Keeffe and O. M. Yaghi, *Chem. Soc. Rev.*, 2009, **38**, 1257-1283.
3. J. L. C. Rowsell and O. M. Yaghi, *Microporous Mesoporous Mat.*, 2004, **73**, 3-14.
4. C. Janiak, *Angew. Chem.-Int. Edit.*, 1997, **36**, 1431-1434.
5. O. M. Yaghi and G. M. Li, *Abstr. Pap. Am. Chem. Soc.*, 1995, **209**, 284-INOR.
6. P. Gómez-Romero and C. Sanchez, Wiley-VCH Verlag GmbH & Co. KGaA, 2004, pp. i-xvii.
7. G. Férey, *Chem. Soc. Rev.*, 2008, **37**, 191-214.
8. B. Moulton and M. J. Zaworotko, *Chem. Rev.*, 2001, **101**, 1629-1658.
9. U. Müeller, M. Schubert, F. Teich, H. Puetter, K. Schierle-Arndt and J. Pastre, *J. Mater. Chem.*, 2006, **16**, 626-636.
10. C. Janiak and J. K. Vieth, *New J. Chem.*, 2010, **34**, 2366-2388.
11. C. Janiak, *Dalton Trans.*, 2003, 2781-2804.
12. A. K. Cheetham, C. N. R. Rao and R. K. Feller, *Chem. Commun.*, 2006, **14**, 4780-4795.
13. N. L. Rosi, M. Eddaoudi, J. Kim, M. O'Keeffe and O. M. Yaghi, *Crystengcomm*, 2002, **4**, 401-404.
14. M. Eddaoudi, J. Kim, N. Rosi, D. Vodak, J. Wachter, M. O'Keeffe and O. M. Yaghi, *Science*, 2002, **295**, 469-472.
15. H. Furukawa, K. E. Cordova, M. O'Keeffe and O. M. Yaghi, *Science*, 2013, **341**.
16. P. Horcajada, R. Gref, T. Baati, P. K. Allan, G. Maurin, P. Couvreur, G. Férey, R. E. Morris and C. Serre, *Chem. Rev.*, 2012, **112**, 1232-1268.
17. E. Coronado and G. Minguez Espallargas, *Chem. Soc. Rev.*, 2013, **42**, 1525-1539.
18. R. J. Kuppler, D. J. Timmons, Q. R. Fang, J. R. Li, T. A. Makal, M. D. Young, D. Q. Yuan, D. Zhao, W. J. Zhuang and H. C. Zhou, *Coord. Chem. Rev.*, 2009, **253**, 3042-3066.
19. W. J. Phang, W. R. Lee, K. Yoo, D. W. Ryu, B. Kim and C. S. Hong, *Angew. Chem.-Int. Edit.*, 2014, **53**, 8383-8387.
20. J. R. Li, J. Sculley and H. C. Zhou, *Chem. Rev.*, 2012, **112**, 869-932.
21. Y. J. Cui, Y. F. Yue, G. D. Qian and B. L. Chen, *Chem. Rev.*, 2012, **112**, 1126-1162.
22. M. D. Allendorf, C. A. Bauer, R. K. Bhakta and R. J. T. Houk, *Chem. Soc. Rev.*, 2009, **38**, 1330-1352.
23. J. Heine and K. Muller-Buschbaum, *Chem. Soc. Rev.*, 2013, **42**, 9232-9242.
24. Z. C. Hu, B. J. Deibert and J. Li, *Chem. Soc. Rev.*, 2014, **43**, 5815-5840.
25. S. L. James, *Chem. Soc. Rev.*, 2003, **32**, 276-288.
26. A. U. Czaja, N. Trukhan and U. Müller, *Chem. Soc. Rev.*, 2009, **38**, 1284-1293.
27. T. R. Cook, Y. R. Zheng and P. J. Stang, *Chem. Rev.*, 2013, **113**, 734-777.
28. M. L. Foo, R. Matsuda and S. Kitagawa, *Chem. Mat.*, 2014, **26**, 310-322.
29. M. Li, D. Li, M. O'Keeffe and O. M. Yaghi, *Chem. Rev.*, 2014, **114**, 1343-1370.
30. N. Stock and S. Biswas, *Chem. Rev.*, 2012, **112**, 933-969.
31. W. G. Lu, Z. W. Wei, Z. Y. Gu, T. F. Liu, J. Park, J. Tian, M. W. Zhang, Q. Zhang, T. Gentle, M. Bosch and H. C. Zhou, *Chem. Soc. Rev.*, 2014, **43**, 5561-5593.
32. Z. Q. Wang and S. M. Cohen, *Chem. Soc. Rev.*, 2009, **38**, 1315-1329.
33. S. Kitagawa, R. Kitaura and S. Noro, *Angew. Chem.-Int. Edit.*, 2004, **43**, 2334-2375.
34. C. J. Kepert, *Chem. Commun.*, 2006, 695-700.
35. N. R. Champness, *Dalton Trans.*, 2006, 877-880.
36. P. M. Forster, A. R. Burbank, C. Livage, G. Férey and A. K. Cheetham, *Chem. Commun.*, 2004, 368-369.
37. W. H. Zhang, Y. Y. Wang, E. K. Lermontova, G. P. Yang, B. Liu, J. C. Jin, Z. Dong and Q. Z. Shi, *Cryst. Growth Des.*, 2010, **10**, 76-84.
38. X. Y. Chen, B. Zhao, W. Shi, J. Xia, P. Cheng, D. Z. Liao, S. P. Yan and Z. H. Jiang, *Chem. Mat.*, 2005, **17**, 2866-2874.

39. D. X. Wang, H. Y. He, X. H. Chen, S. Y. Feng, Y. Z. Niu and D. F. Sun, *Crystengcomm*, 2010, **12**, 1041-1043.
40. J. Y. Wu, T. C. Chao and M. S. Zhong, *Cryst. Growth Des.*, 2013, **13**, 2953-2964.
41. H. L. Li, C. E. Davis, T. L. Groy, D. G. Kelley and O. M. Yaghi, *J. Am. Chem. Soc.*, 1998, **120**, 2186-2187.
42. L. Pineiro-Lopez, Z. Arcis-Castillo, M. C. Munoz and J. A. Real, *Cryst. Growth Des.*, 2014, **14**, 6311-6319.
43. S. L. Qiu and G. S. Zhu, *Coord. Chem. Rev.*, 2009, **253**, 2891-2911.
44. L. J. Shen, W. M. Wu, R. W. Liang, R. Lin and L. Wu, *Nanoscale*, 2013, **5**, 9374-9382.
45. C. Serre, F. Millange, C. Thouvenot, M. Nogues, G. Marsolier, D. Louer and G. Férey, *J. Am. Chem. Soc.*, 2002, **124**, 13519-13526.
46. Y. F. Zhang, X. J. Bo, A. Nsabimana, C. Han, M. Li and L. P. Guo, *J. Mater. Chem. A*, 2015, **3**, 732-738.
47. T. R. C. Van Assche, G. Desmet, R. Ameloot, D. E. De Vos, H. Terryn and J. F. M. Denayer, *Microporous Mesoporous Mat.*, 2012, **158**, 209-213.
48. N. Campagnol, E. R. Souza, D. E. De Vos, K. Binnemans and J. Fransaer, *Chem. Commun.*, 2014, **50**, 12545-12547.
49. L. R. MacGillivray, *Metal-Organic Frameworks: Design and Application*, John Wiley & Sons, 2010.
50. A. Pichon, A. Lazuen-Garay and S. L. James, *Crystengcomm*, 2006, **8**, 211-214.
51. S. L. James, C. J. Adams, C. Bolm, D. Braga, P. Collier, T. Friscic, F. Grepioni, K. D. M. Harris, G. Hyett, W. Jones, A. Krebs, J. Mack, L. Maini, A. G. Orpen, I. P. Parkin, W. C. Shearouse, J. W. Steed and D. C. Waddell, *Chem. Soc. Rev.*, 2012, **41**, 413-447.
52. M. Y. Masoomi, A. Morsali and P. C. Junk, *Crystengcomm*, 2015, **17**, 686-692.
53. S. H. Jhung, J. W. Yoon, J. S. Hwang, A. K. Cheetham and J. S. Chang, *Chem. Mat.*, 2005, **17**, 4455-4460.
54. S. H. Jhung, J. S. Chang, J. S. Hwang and S. E. Park, *Microporous Mesoporous Mat.*, 2003, **64**, 33-39.
55. Y. K. Hwang, J. S. Chang, S. E. Park, D. S. Kim, Y. U. Kwon, S. H. Jhung, J. S. Hwang and M. S. Park, *Angew. Chem.-Int. Edit.*, 2005, **44**, 556-560.
56. Z. Ni and R. I. Masel, *J. Am. Chem. Soc.*, 2006, **128**, 12394-12395.
57. R. Sabouni, H. Kazemian and S. Rohani, *Chem. Eng. Technol.*, 2012, **35**, 1085-1092.
58. A. Morsali, H. H. Monfared and C. Janiak, *Ultrason. Sonochem.*, 2015, **23**, 208-211.
59. D. W. Jung, D. A. Yang, J. Kim and W. S. Ahn, *Dalton Trans.*, 2010, **39**, 2883-2887.
60. W. J. Son, J. Kim and W. S. Ahn, *Chem. Commun.*, 2008, 6336-6338.
61. E. Haque, N. A. Khan, J. H. Park and S. H. Jhung, *Chem.-Eur. J.*, 2010, **16**, 1046-1052.
62. L. N. Jin, Q. Liu and W. Y. Sun, *Crystengcomm*, 2014, **16**, 3816-3828.
63. A. C. Sudik, A. P. Cote, A. G. Wong-Foy, M. O'Keeffe and O. M. Yaghi, *Angew. Chem.-Int. Edit.*, 2006, **45**, 2528-2533.
64. D. J. Tranchemontagne, J. R. Hunt and O. M. Yaghi, *Tetrahedron*, 2008, **64**, 8553-8557.
65. I. Imaz, J. Hernando, D. Ruiz-Molina and D. MasPOCH, *Angew. Chem.-Int. Edit.*, 2009, **48**, 2325-2329.
66. L. Y. Wang, S. Lu, Y. X. Zhou, X. D. Guo, Y. L. Lu, J. He and D. G. Evans, *Chem. Commun.*, 2011, **47**, 11002-11004.
67. A. E. Platero-Prats, A. B. Gomez, L. Samain, X. D. Zou and B. Martin-Matute, *Chem.-Eur. J.*, 2015, **21**, 861-866.
68. M. P. Suh, H. J. Park, T. K. Prasad and D. W. Lim, *Chem. Rev.*, 2012, **112**, 782-835.
69. Y. B. He, W. Zhou, G. D. Qian and B. L. Chen, *Chem. Soc. Rev.*, 2014, **43**, 5657-5678.
70. K. Sumida, D. L. Rogow, J. A. Mason, T. M. McDonald, E. D. Bloch, Z. R. Herm, T. H. Bae and J. R. Long, *Chem. Rev.*, 2012, **112**, 724-781.
71. E. Barea, C. Montoro and J. A. R. Navarro, *Chem. Soc. Rev.*, 2014, **43**, 5419-5430.
72. M. Yoon, R. Srirambalaji and K. Kim, *Chem. Rev.*, 2012, **112**, 1196-1231.
73. A. Morozan and F. Jaouen, *Energy Environ. Sci.*, 2012, **5**, 9269-9290.

74. G. Ferey, F. Millange, M. Morcrette, C. Serre, M. L. Doublet, J. M. Greneche and J. M. Tarascon, *Angew. Chem.-Int. Edit.*, 2007, **46**, 3259-3263.
75. K. D. Demadis, M. Papadaki, R. G. Raptis and H. Zhao, *Chem. Mat.*, 2008, **20**, 4835-4846.
76. See DOE MOVE program at <https://arpa-e-foa.energy.gov/>.
77. Y. Peng, V. Krungleviciute, I. Eryazici, J. T. Hupp, O. K. Farha and T. Yildirim, *J. Am. Chem. Soc.*, 2013, **135**, 11887-11894.
78. H. W. Langmi, J. W. Ren, B. North, M. Mathe and D. Bessarabov, *Electrochim. Acta*, 2014, **128**, 368-392.
79. J. L. C. Rowsell and O. M. Yaghi, *J. Am. Chem. Soc.*, 2006, **128**, 1304-1315.
80. T. Loiseau, L. Lecroq, C. Volkringer, J. Marrot, G. Férey, M. Haouas, F. Taulelle, S. Bourrelly, P. L. Llewellyn and M. Latroche, *J. Am. Chem. Soc.*, 2006, **128**, 10223-10230.
81. K. S. Park, Z. Ni, A. P. Cote, J. Y. Choi, R. D. Huang, F. J. Uribe-Romo, H. K. Chae, M. O'Keeffe and O. M. Yaghi, *Proc. Natl. Acad. Sci. U. S. A.*, 2006, **103**, 10186-10191.
82. X. Lin, I. Telepeni, A. J. Blake, A. Dailly, C. M. Brown, J. M. Simmons, M. Zoppi, G. S. Walker, K. M. Thomas, T. J. Mays, P. Hubberstey, N. R. Champness and M. Schroder, *J. Am. Chem. Soc.*, 2009, **131**, 2159-2171.
83. S. Q. Ma, J. Eckert, P. M. Forster, J. W. Yoon, Y. K. Hwang, J. S. Chang, C. D. Collier, J. B. Parise and H. C. Zhou, *J. Am. Chem. Soc.*, 2008, **130**, 15896-15902.
84. Y. G. Lee, H. R. Moon, Y. E. Cheon and M. P. Suh, *Angew. Chem.-Int. Edit.*, 2008, **47**, 7741-7745.
85. D. J. Tranchemontagne, K. S. Park, H. Furukawa, J. Eckert, C. B. Knobler and O. M. Yaghi, *J. Phys. Chem. C*, 2012, **116**, 13143-13151.
86. M. Bosch, M. W. Zhang, D. W. Feng, S. Yuan, X. Wang, Y. P. Chen and H. C. Zhou, *APL Mater.*, 2014, **2**.
87. D. W. Lim, S. A. Chyun and M. P. Suh, *Angew. Chem.-Int. Edit.*, 2014, **53**, 7819-7822.
88. K. L. Mulfort, O. K. Farha, C. L. Stern, A. A. Sarjeant and J. T. Hupp, *J. Am. Chem. Soc.*, 2009, **131**, 3866-3868.
89. P. A. Szilagy, I. Weinrauch, H. Oh, M. Hirscher, J. Juan-Alcaniz, P. Serra-Crespo, M. de Respinis, B. J. Trzesniewski, F. Kapteijn, H. Geerlings, J. Gascon, B. Dam, A. Grzech and R. van de Krol, *J. Phys. Chem. C*, 2014, **118**, 19572-19579.
90. S. J. Yang, J. H. Cho, K. Lee, T. Kim and C. R. Park, *Chem. Mat.*, 2010, **22**, 6138-6145.
91. S. H. Yang, X. Lin, A. J. Blake, G. S. Walker, P. Hubberstey, N. R. Champness and M. Schröder, *Nat. Chem.*, 2009, **1**, 487-493.
92. D. Saha and S. G. Deng, *Int. J. Hydrog. Energy*, 2009, **34**, 2670-2678.
93. R. Bhattacharyya and S. Mohan, *Renew. Sust. Energ. Rev.*, 2015, **41**, 872-883.
94. J. L. Belof, A. C. Stern, M. Eddaoudi and B. Space, *J. Am. Chem. Soc.*, 2007, **129**, 15202-15210.
95. Y. L. Liu, J. F. Eubank, A. J. Cairns, J. Eckert, V. C. Kravtsov, R. Luebke and M. Eddaoudi, *Angew. Chem.-Int. Edit.*, 2007, **46**, 3278-3283.
96. G. Q. Li, H. Kobayashi, J. M. Taylor, R. Ikeda, Y. Kubota, K. Kato, M. Takata, T. Yamamoto, S. Toh, S. Matsumura and H. Kitagawa, *Nat. Mater.*, 2014, **13**, 802-806.
97. J. Kim, S. Yeo, J. D. Jeon and S. Y. Kwak, *Microporous Mesoporous Mat.*, 2015, **202**, 8-15.
98. S. N. Klyamkin, S. V. Chuvikov, N. V. Maletskaya, E. V. Kogan, V. P. Fedin, K. A. Kovalenko and D. N. Dybtsev, *Int. J. Energy Res.*, 2014, **38**, 1562-1570.
99. J. W. Ren, N. M. Musyoka, H. W. Langmi, B. C. North, M. Mathe and X. D. Kang, *Int. J. Hydrog. Energy*, 2014, **39**, 14912-14917.
100. V. C. Menon and S. Komarneni, *J. Porous Mat.*, 1998, **5**, 43-58.
101. D. Lozano-Castello, J. Alcaniz-Monge, M. A. de la Casa-Lillo, D. Cazorla-Amoros and A. Linares-Solano, *Fuel*, 2002, **81**, 1777-1803.
102. K. Konstas, T. Osl, Y. X. Yang, M. Batten, N. Burke, A. J. Hill and M. R. Hill, *J. Mater. Chem.*, 2012, **22**, 16698-16708.
103. G. Barin, V. Krungleviciute, D. A. Gomez-Gualdrón, A. A. Sarjeant, R. Q. Snurr, J. T. Hupp, T. Yildirim and O. K. Farha, *Chem. Mat.*, 2014, **26**, 1912-1917.
104. Y. B. He, W. Zhou, T. Yildirim and B. L. Chen, *Energy Environ. Sci.*, 2013, **6**, 2735-2744.
105. S. J. Lee and Y. S. Bae, *J. Phys. Chem. C*, 2014, **118**, 19833-19841.

106. S. Noro, S. Kitagawa, M. Kondo and K. Seki, *Angew. Chem.-Int. Edit.*, 2000, **39**, 2082-2084.
107. I. Senkowska and S. Kaskel, *Microporous Mesoporous Mat.*, 2008, **112**, 108-115.
108. Z. Y. Guo, H. Wu, G. Srinivas, Y. M. Zhou, S. C. Xiang, Z. X. Chen, Y. T. Yang, W. Zhou, M. O'Keeffe and B. L. Chen, *Angew. Chem.-Int. Edit.*, 2011, **50**, 3178-3181.
109. Y. Peng, G. Srinivas, C. E. Wilmer, I. Eryazici, R. Q. Snurr, J. T. Hupp, T. Yildirim and O. K. Farha, *Chem. Commun.*, 2013, **49**, 2992-2994.
110. C. E. Wilmer, O. K. Farha, T. Yildirim, I. Eryazici, V. Krungleviciute, A. A. Sarjeant, R. Q. Snurr and J. T. Hupp, *Energy Environ. Sci.*, 2013, **6**, 1158-1163.
111. Y. Yan, M. Suyetin, E. Bichoutskaia, A. J. Blake, D. R. Allan, S. A. Barnett and M. Schröder, *Chem. Sci.*, 2013, **4**, 1731-1736.
112. S. Q. Ma, D. F. Sun, J. M. Simmons, C. D. Collier, D. Q. Yuan and H. C. Zhou, *J. Am. Chem. Soc.*, 2008, **130**, 1012-1016.
113. F. Gandara, H. Furukawa, S. Lee and O. M. Yaghi, *J. Am. Chem. Soc.*, 2014, **136**, 5271-5274.
114. J. Liu, P. K. Thallapally, B. P. McGrail and D. R. Brown, *Chem. Soc. Rev.*, 2012, **41**, 2308-2322.
115. Q. A. Wang, J. Z. Luo, Z. Y. Zhong and A. Borgna, *Energy Environ. Sci.*, 2011, **4**, 42-55.
116. Z. J. Zhang, Y. G. Zhao, Q. H. Gong, Z. Li and J. Li, *Chem. Commun.*, 2013, **49**, 653-661.
117. D. M. D'Alessandro, B. Smit and J. R. Long, *Angew. Chem.-Int. Edit.*, 2010, **49**, 6058-6082.
118. W. M. Xuan, C. F. Zhu, Y. Liu and Y. Cui, *Chem. Soc. Rev.*, 2012, **41**, 1677-1695.
119. E. Lopez-Maya, C. Montoro, V. Colombo, E. Barea and J. A. R. Navarro, *Adv. Funct. Mater.*, 2014, **24**, 6130-6135.
120. V. Colombo, C. Montoro, A. Maspero, G. Palmisano, N. Masciocchi, S. Galli, E. Barea and J. A. R. Navarro, *J. Am. Chem. Soc.*, 2012, **134**, 12830-12843.
121. S. S. Chen, M. Chen, S. Takamizawa, P. Wang, G. C. Lv and W. Y. Sun, *Chem. Commun.*, 2011, **47**, 4902-4904.
122. S. Bordiga, L. Regli, F. Bonino, E. Groppo, C. Lamberti, B. Xiao, P. S. Wheatley, R. E. Morris and A. Zecchina, *Phys. Chem. Chem. Phys.*, 2007, **9**, 2676-2685.
123. A. R. Millward and O. M. Yaghi, *J. Am. Chem. Soc.*, 2005, **127**, 17998-17999.
124. P. L. Llewellyn, S. Bourrelly, C. Serre, A. Vimont, M. Daturi, L. Hamon, G. De Weireld, J. S. Chang, D. Y. Hong, Y. K. Hwang, S. H. Jhung and G. Férey, *Langmuir*, 2008, **24**, 7245-7250.
125. O. K. Farha, A. O. Yazaydin, I. Eryazici, C. D. Malliakas, B. G. Hauser, M. G. Kanatzidis, S. T. Nguyen, R. Q. Snurr and J. T. Hupp, *Nat. Chem.*, 2010, **2**, 944-948.
126. B. Mu, P. M. Schoenecker and K. S. Walton, *J. Phys. Chem. C*, 2010, **114**, 6464-6471.
127. H. Furukawa, N. Ko, Y. B. Go, N. Aratani, S. B. Choi, E. Choi, A. O. Yazaydin, R. Q. Snurr, M. O'Keeffe, J. Kim and O. M. Yaghi, *Science*, 2010, **329**, 424-428.
128. B. Wang, A. P. Cote, H. Furukawa, M. O'Keeffe and O. M. Yaghi, *Nature*, 2008, **453**, 207-U206.
129. D. Britt, H. Furukawa, B. Wang, T. G. Glover and O. M. Yaghi, *Proc. Natl. Acad. Sci. U. S. A.*, 2009, **106**, 20637-20640.
130. J. R. Li, Y. Tao, Q. Yu, X. H. Bu, H. Sakamoto and S. Kitagawa, *Chem.-Eur. J.*, 2008, **14**, 2771-2776.
131. A. C. Kizzie, A. G. Wong-Foy and A. J. Matzger, *Langmuir*, 2011, **27**, 6368-6373.
132. L. Bastin, P. S. Barcia, E. J. Hurtado, J. A. C. Silva, A. E. Rodrigues and B. L. Chen, *J. Phys. Chem. C*, 2008, **112**, 1575-1581.
133. K. Nakagawa, D. Tanaka, S. Horike, S. Shimomura, M. Higuchi and S. Kitagawa, *Chem. Commun.*, 2010, **46**, 4258-4260.
134. Z. J. Zhang, Z. Z. Yao, S. C. Xiang and B. L. Chen, *Energy Environ. Sci.*, 2014, **7**, 2868-2899.
135. N. T. T. Nguyen, H. Furukawa, F. Gandara, H. T. Nguyen, K. E. Cordova and O. M. Yaghi, *Angew. Chem.-Int. Edit.*, 2014, **53**, 10645-10648.
136. W. Y. Huang, X. Zhou, Q. B. Xia, J. J. Peng, H. H. Wang and Z. Li, *Ind. Eng. Chem. Res.*, 2014, **53**, 11176-11184.
137. X.-H. Liu, J.-G. Ma, Z. Niu, G.-M. Yang and P. Cheng, *Angew. Chem.-Int. Edit.*, 2015, **54**, 988-991.
138. Q. Xin, J. Ouyang, T. Liu, Z. Li, Z. Li, Y. Liu, S. Wang, H. Wu, Z. Jiang and X. Cao, *ACS Appl. Mater. Interfaces*, 2015, **7**, 1065-1077.

139. S. Y. Lim, J. Choi, H. Y. Kim, Y. Kim, S. J. Kim, Y. S. Kang and J. Won, *J. Membr. Sci.*, 2014, **467**, 67-72.
140. T. Rodenas, M. van Dalen, P. Serra-Crespo, F. Kapteijn and J. Gascon, *Microporous Mesoporous Mat.*, 2014, **192**, 35-42.
141. T. Rodenas, M. van Dalen, E. Garcia-Perez, P. Serra-Crespo, B. Zornoza, F. Kapteijn and J. Gascon, *Adv. Funct. Mater.*, 2014, **24**, 249-256.
142. A. S. Huang, Q. Liu, N. Y. Wang and J. Caro, *Microporous Mesoporous Mat.*, 2014, **192**, 18-22.
143. F. Dorosti, M. Omidkhah and R. Abedini, *Chem. Eng. Res. Des.*, 2014, **92**, 2439-2448.
144. N. A. Khan, Z. Hasan and S. H. Jung, *J. Hazard. Mater.*, 2013, **244**, 444-456.
145. D. Britt, D. Tranchemontagne and O. M. Yaghi, *Proc. Natl. Acad. Sci. U. S. A.*, 2008, **105**, 11623-11627.
146. T. G. Glover, G. W. Peterson, B. J. Schindler, D. Britt and O. Yaghi, *Chem. Eng. Sci.*, 2011, **66**, 163-170.
147. Z. Hasan, J. Jeon and S. H. Jung, *J. Hazard. Mater.*, 2012, **209**, 151-157.
148. Y. Li, L. J. Wang, H. L. Fan, J. Shanguan, H. Wang and J. Mi, *Energ. Fuel.*, 2015, **29**, 298-304.
149. M. T. Luebbbers, T. J. Wu, L. J. Shen and R. I. Masel, *Langmuir*, 2010, **26**, 11319-11329.
150. N. M. Padial, E. Q. Procopio, C. Montoro, E. Lopez, J. E. Oltra, V. Colombo, A. Maspero, N. Masciocchi, S. Galli, I. Senkovska, S. Kaskel, E. Barea and J. A. R. Navarro, *Angew. Chem.-Int. Edit.*, 2013, **52**, 8290-8294.
151. S. Galli, N. Masciocchi, V. Colombo, A. Maspero, G. Palmisano, F. J. Lopez-Garzon, M. Domingo-Garcia, I. Fernandez-Morales, E. Barea and J. A. R. Navarro, *Chem. Mat.*, 2010, **22**, 1664-1672.
152. C. Montoro, F. Linares, E. Q. Procopio, I. Senkovska, S. Kaskel, S. Galli, N. Masciocchi, E. Barea and J. A. R. Navarro, *J. Am. Chem. Soc.*, 2011, **133**, 11888-11891.
153. G. W. Peterson, J. B. DeCoste, F. Fatollahi-Fard and D. K. Britt, *Ind. Eng. Chem. Res.*, 2014, **53**, 701-707.
154. A. Roy, A. K. Srivastava, B. Singh, D. Shah, T. H. Mahato, P. K. Gutch and A. K. Halve, *J. Porous Mat.*, 2013, **20**, 1103-1109.
155. B. Supronowicz, A. Mavrandonakis and T. Heine, *J. Phys. Chem. C*, 2013, **117**, 14570-14578.
156. K. Yang, Q. Sun, F. Xue and D. H. Lin, *J. Hazard. Mater.*, 2011, **195**, 124-131.
157. C. Y. Huang, M. Song, Z. Y. Gu, H. F. Wang and X. P. Yan, *Environ. Sci. Technol.*, 2011, **45**, 4490-4496.
158. J. A. Bernstein, N. Alexis, H. Bacchus, I. L. Bernstein, P. Fritz, E. Horner, N. Li, S. Mason, A. Nel, J. Oullette, K. Reijula, T. Reponen, J. Seltzer, A. Smith and S. M. Tarlo, *J. Allergy Clin. Immunol.*, 2008, **121**, 585-591.
159. P. Wolkoff, C. K. Wilkins, P. A. Clausen and G. D. Nielsen, *Indoor Air*, 2006, **16**, 7-19.
160. I. Ahmed, N. A. Khan and S. H. Jung, *Inorg. Chem.*, 2013, **52**, 14155-14161.
161. M. Tu and R. A. Fischer, *J. Mater. Chem. A*, 2014, **2**, 2018-2022.
162. X. Q. Zou, J. M. Goupil, S. Thomas, F. Zhang, G. S. Zhu, V. Valtchev and S. Mintova, *J. Phys. Chem. C*, 2012, **116**, 16593-16600.
163. O. Shekhah, A. Cadiou and M. Eddaoudi, *Crystengcomm*, 2015, **17**, 290-294.
164. A. H. Khoshaman and B. Bahreyni, *Sens. Actuator B-Chem.*, 2012, **162**, 114-119.
165. H. Yamagiwa, S. Sato, T. Fukawa, T. Ikehara, R. Maeda, T. Mihara and M. Kimura, *Sci Rep*, 2014, **4**.
166. Q. R. Fang, D. Q. Yuan, J. Sculley, J. R. Li, Z. B. Han and H. C. Zhou, *Inorg. Chem.*, 2010, **49**, 11637-11642.
167. K. K. Tanabe and S. M. Cohen, *Angew. Chem.-Int. Edit.*, 2009, **48**, 7424-7427.
168. Y. Y. Pan, B. Z. Yuan, Y. W. Li and D. H. He, *Chem. Commun.*, 2010, **46**, 2280-2282.
169. S. Ribeiro, A. D. S. Barbosa, A. C. Gomes, M. Pillinger, I. S. Goncalves, L. Cunha-Silva and S. S. Balula, *Fuel Process. Technol.*, 2013, **116**, 350-357.
170. T. Ishida, M. Nagaoka, T. Akita and M. Haruta, *Chem.-Eur. J.*, 2008, **14**, 8456-8460.
171. B. Z. Yuan, Y. Y. Pan, Y. W. Li, B. L. Yin and H. F. Jiang, *Angew. Chem.-Int. Edit.*, 2010, **49**, 4054-4058.

172. A. Aijaz, A. Karkamkar, Y. J. Choi, N. Tsumori, E. Ronnebro, T. Autrey, H. Shioyama and Q. Xu, *J. Am. Chem. Soc.*, 2012, **134**, 13926-13929.
173. S. Hasegawa, S. Horike, R. Matsuda, S. Furukawa, K. Mochizuki, Y. Kinoshita and S. Kitagawa, *J. Am. Chem. Soc.*, 2007, **129**, 2607-2614.
174. O. R. Evans, H. L. Ngo and W. B. Lin, *J. Am. Chem. Soc.*, 2001, **123**, 10395-10396.
175. F. J. Song, C. Wang, J. M. Falkowski, L. Q. Ma and W. B. Lin, *J. Am. Chem. Soc.*, 2010, **132**, 15390-15398.
176. K. Gedrich, M. Heitbaum, A. Notzon, I. Senkovska, R. Frohlich, J. Getzschmann, U. Mueller, F. Glorius and S. Kaskel, *Chem.-Eur. J.*, 2011, **17**, 2099-2106.
177. A. G. Hu, H. L. Ngo and W. B. Lin, *J. Am. Chem. Soc.*, 2003, **125**, 11490-11491.
178. H. H. Fei, J. W. Shin, Y. S. Meng, M. Adelhardt, J. Sutter, K. Meyer and S. M. Cohen, *J. Am. Chem. Soc.*, 2014, **136**, 4965-4973.
179. S. M. F. Vilela, A. D. G. Firmino, R. F. Mendes, J. A. Fernandes, D. Ananias, A. A. Valente, H. Ott, L. D. Carlos, J. Rocha, J. P. C. Tome and F. A. A. Paz, *Chem. Commun.*, 2013, **49**, 6400-6402.
180. Y. Z. Chen, Q. Xu, S. H. Yu and H. L. Jiang, *Small*, 2015, **11**, 71-76.
181. J. Song, Z. Luo, D. K. Britt, H. Furukawa, O. M. Yaghi, K. I. Hardcastle and C. L. Hill, *J. Am. Chem. Soc.*, 2011, **133**, 16839-16846.
182. B. Joarder, A. V. Desai, P. Samanta, S. Mukherjee and S. K. Ghosh, *Chem.-Eur. J.*, 2015, **21**, 965-969.
183. X. G. Liu, H. Wang, B. Chen, Y. Zou, Z. G. Gu, Z. J. Zhao and L. Shen, *Chem. Commun.*, 2015, **51**, 1677-1680.
184. D. P. Yan, Y. Q. Tang, H. Y. Lin and D. Wang, *Sci Rep*, 2014, **4**.
185. Y. F. Yue, A. J. Binder, R. J. Song, Y. J. Cui, J. H. Chen, D. K. Hensley and S. Dai, *Dalton Trans.*, 2014, **43**, 17893-17898.
186. M. Zhang, G. X. Feng, Z. G. Song, Y. P. Zhou, H. Y. Chao, D. Q. Yuan, T. T. Y. Tan, Z. G. Guo, Z. G. Hu, B. Z. Tang, B. Liu and D. Zhao, *J. Am. Chem. Soc.*, 2014, **136**, 7241-7244.
187. G. Y. Wang, C. Song, D. M. Kong, W. J. Ruan, Z. Chang and Y. Li, *J. Mater. Chem. A*, 2014, **2**, 2213-2220.
188. B. L. Chen, L. B. Wang, F. Zapata, G. D. Qian and E. B. Lobkovsky, *J. Am. Chem. Soc.*, 2008, **130**, 6718-6719.
189. Q. B. Bo, H. T. Zhang, H. Y. Wang, J. L. Miao and Z. W. Zhang, *Chem.-Eur. J.*, 2014, **20**, 3712-3723.
190. Y. Lu, B. Yan and J. L. Liu, *Chem. Commun.*, 2014, **50**, 9969-9972.
191. Z. H. Xiang, C. Q. Fang, S. H. Leng and D. P. Cao, *J. Mater. Chem. A*, 2014, **2**, 7662-7665.
192. B. V. Harbuzaru, A. Corma, F. Rey, J. L. Jorda, D. Ananias, L. D. Carlos and J. Rocha, *Angew. Chem.-Int. Edit.*, 2009, **48**, 6476-6479.
193. Y. Zhou, B. Yan and F. Lei, *Chem. Commun.*, 2014, **50**, 15235-15238.
194. Y. Takashima, V. M. Martinez, S. Furukawa, M. Kondo, S. Shimomura, H. Uehara, M. Nakahama, K. Sugimoto and S. Kitagawa, *Nat. Commun.*, 2011, **2**.
195. E. D. Bloch, D. Britt, C. Lee, C. J. Doonan, F. J. Uribe-Romo, H. Furukawa, J. R. Long and O. M. Yaghi, *J. Am. Chem. Soc.*, 2010, **132**, 14382-14384.
196. I. R. Fernando, S. Jianrattanasawat, N. Daskalakis, K. D. Demadis and G. Mezei, *Crystengcomm*, 2012, **14**, 908-919.
197. I. R. Fernando, N. Daskalakis, K. D. Demadis and G. Mezei, *New J. Chem.*, 2010, **34**, 221-235.
198. S. E. H. Etaiw, A. S. Fouda, S. N. Abdou and M. M. El-bendary, *Corrosion Sci.*, 2011, **53**, 3657-3665.
199. A. Mesbah, S. Jacques, E. Rocca, M. Francois and J. Steinmetz, *Eur. J. Inorg. Chem.*, 2011, 1315-1321.
200. K. D. Demadis, S. D. Katarachia and M. Koutmos, *Inorg. Chem. Commun.*, 2005, **8**, 254-258.
201. K. D. Demadis, M. Papadaki, R. G. Raptis and H. Zhao, *J. Solid State Chem.*, 2008, **181**, 679-683.
202. B. Yilmaz, N. Trukhan and U. Müller, *Chinese J. Catal.*, 2012, **33**, 3-10.
203. M. Gaab, N. Trukhan, S. Maurer, R. Gummaraju and U. Müller, *Microporous Mesoporous Mat.*, 2012, **157**, 131-136.

204. S. S.-Y. Chui, S. M.-F. Lo, J. P. H. Charmant, A. G. Orpen and I. D. Williams, *Science*, 1999, **283**, 1148-1150.
205. T. Loiseau, C. Serre, C. Huguenard, G. Fink, F. Taulelle, M. Henry, T. Bataille and G. Férey, *Chem.-Eur. J.*, 2004, **10**, 1373-1382.
206. *United States of America Pat.*, US8197619B1, 2012.
207. A. U. Czaja, N. Trukhan and U. Muller, *Chem. Soc. Rev.*, 2009, **38**, 1284-1293.
208. *Germany Pat.*, WO2007131955A1, 2007.
209. *Germany Pat.*, WO2010106121A1, 2010.
210. H. X. Deng, S. Grunder, K. E. Cordova, C. Valente, H. Furukawa, M. Hmadeh, F. Gandara, A. C. Whalley, Z. Liu, S. Asahina, H. Kazumori, M. O'Keeffe, O. Terasaki, J. F. Stoddart and O. M. Yaghi, *Science*, 2012, **336**, 1018-1023.
211. *Germany Pat.*, WO2012042410A1, 2012.
212. H. Furukawa, M. A. Miller and O. M. Yaghi, *J. Mater. Chem.*, 2007, **17**, 3197-3204.
213. in *Remise des Prix Pierre Potier et ChemStart'UP 2012*, France Chemie - Fédération Française pour les sciences de la Chimie, 2012.
214. *South Korea Pat.*, WO2011062412A2, 2013.
215. *Norway Pat.*, WO2009133366A2, 2012.
216. *European Patent Database* <http://www.epo.org/>, Accessed 02 March 2015.
217. *United States of America Pat.*, US5648508A, 1997.
218. M. Jacoby, *Chem. Eng. News*, 2008, **86**, 13-16.
219. M. Jacoby, *Chem. Eng. News*, 2013, **91**, 34-35.
220. *United States of America Pat.*, US20110142752A1, 2011.
221. *United States of America Pat.*, US20110142750A1, 2011.
222. J. Clark, in *eMercedesBenz - online magazine*, <http://www.mercedesbenz.com/autos/mercedes-benz/concept-vehicles/mercedes-benz-fl125-research-vehicle-technology/>, 2011.
223. *United States of America Pat.*, US8658319B2, 2014.
224. *United States of America Pat.*, US2015044553A1, 2015.
225. *France Pat.*, WO2014009611A1, 2014.
226. *France Pat.*, WO2012089716A1, 2012.
227. *France Pat.*, WO2012004328A1, 2012.
228. *Functional Metal Organic Frameworks as Heterogeneous Catalysts - MOFCAT project, Final Report*, cordis.europa.eu/project/rcn/80027_en.html, Accessed 02 March 2015.
229. L. Mitchell, B. Gonzalez-Santiago, J. P. S. Mowat, M. E. Gunn, P. Williamson, N. Acerbi, M. L. Clarke and P. A. Wright, *Catal. Sci. Technol.*, 2013, **3**, 606-617.
230. *Great Britain Pat.*, WO2013160683A1, 2013.
231. *Great Britain Pat.*, WO2014114948A1, 2014.
232. A. Dhakshinamoorthy, M. Alvaro and H. Garcia, *J. Catal.*, 2012, **289**, 259-265.
233. S. Biswas, M. Maes, A. Dhakshinamoorthy, M. Feyand, D. E. De Vos, H. Garcia and N. Stock, *J. Mater. Chem.*, 2012, **22**, 10200-10209.
234. M. de Miguel, F. Ragon, T. Devic, C. Serre, P. Horcajada and H. Garcia, *Chemphyschem*, 2012, **13**, 3651-3654.
235. A. Micek-Ilnicka and B. Gil, *Dalton Trans.*, 2012, **41**, 12624-12629.
236. M. A. Moreira, J. C. Santos, A. F. P. Ferreira, J. M. Loureiro, F. Ragon, P. Horcajada, K.-E. Shim, Y.-K. Hwang, U. H. Lee, J.-S. Chang, C. Serre and A. E. Rodrigues, *Langmuir*, 2012, **28**, 5715-5723.
237. M. A. Moreira, J. C. Santos, A. F. P. Ferreira, J. M. Loureiro, F. Ragon, P. Horcajada, P. G. Yot, C. Serre and A. E. Rodrigues, *Langmuir*, 2012, **28**, 3494-3502.
238. M. G. Plaza, A. M. Ribeiro, A. Ferreira, J. C. Santos, Y. K. Hwang, Y. K. Seo, U. H. Lee, J. S. Chang, J. M. Loureiro and A. E. Rodrigues, *Microporous Mesoporous Mat.*, 2012, **153**, 178-190.
239. M. G. Plaza, A. M. Ribeiro, A. Ferreira, J. C. Santos, U. H. Lee, J.-S. Chang, J. M. Loureiro and A. E. Rodrigues, *Sep. Purif. Technol.*, 2012, **90**, 109-119.
240. S. Wuttke, P. Bazin, A. Vimont, C. Serre, Y.-K. Seo, Y. K. Hwang, J.-S. Chang, G. Férey and M. Daturi, *Chem.-Eur. J.*, 2012, **18**, 11959-11967.
241. I. Casely, *Johnson Matthey Technol. Rev.*, 2014, **58**, 205-211.

242. M. Rose, B. Böhringer, M. Jolly, R. Fischer and S. Kaskel, *Adv. Eng. Mater.*, 2011, **13**, 356-360.
243. *Germany Pat.*, WO2012156436A1, 2012.
244. *Germany Pat.*, DE102009042643A1, 2011.
245. *Iran Pat.*, US20120237697A1, 2012.
246. *Nanoporous Metal-Organic Frameworks for production (nanoMOF) - Project Final Report*, http://cordis.europa.eu/project/rcn/92877_en.html, Accessed 02 March 2015.
247. J. B. DeCoste and G. W. Peterson, *Chem. Rev.*, 2014, **114**, 5695-5727.
248. *United States of America Pat.*, US8883676B1, 2014.
249. *United States of America Pat.*, WO2007035596A2, 2007.
250. *Germany Pat.*, WO2010106105A2, 2012.
251. Z. Wang and S. M. Cohen, *Chem. Soc. Rev.*, 2009, **38**, 1315-1329.
252. J. L. C. Rowsell and O. M. Yaghi, *Angew. Chem.-Int. Edit.*, 2005, **44**, 4670-4679.
253. J. Ren, H. W. Langmi, B. C. North and M. Mathe, *Int. J. Energy Res.*, 2015, **39**, 607-620.
254. J. Ren, N. M. Musyoka, H. W. Langmi, A. Swartbooi, B. C. North and M. Mathe, *Int. J. Hydrog. Energy*, 2015, **40**, 4617-4622.

Table 1

Table 1 - Advantages (↑) and disadvantages (↓) that must be taken into account before the preparation of MOF materials.

Synthetic Method	Advantages/Disadvantages	References
Slow diffusion	↑ It allows, normally, the preparation of MOFs as large single-crystals (fundamental for X-ray diffraction studies); ↑ Ambient conditions (<i>e.g.</i> , pressure and temperature) or low temperatures are usually employed;	38-42
	↓ Very slow process, taking several days, weeks or even months; ↓ Preparation of small amounts of the desired materials.	
Hydro(solvo)thermal	↑ Large operating temperature regime (<i>i.e.</i> , between 80 and 250 °C); ↑ Possibility to perform heating and cooling temperature ramps to help crystal growth; ↑ Easy industrial transposition;	43-46
	↓ Implies high costs to purchase pressure-sealed metal vessels and heating ovens; ↓ High energy consumption; ↓ Reactions take from few to several days.	
Electrochemical	↑ Used for the industrial production of the HKUST-1 MOF material (under the name Basolite™ C300); ↑ Fast, clean synthetic approach;	9, 47-48
	↓ Besides the preparation of HKUST-1 no other MOFs have been reported using this method.	
Mechanochemical	↑ Solvent-free synthetic method; ↑ Pressure and temperature are not required, being only used mechanochemical force;	49-52
	↓ Difficult to isolate single-crystals for X-ray diffraction studies; ↓ Secondary phases are usually obtained.	
Microwave-assisted heating	↑ Simple and energy efficient approach; ↑ Reduction of crystallization times and improvement of yields; ↑ Possibility to control morphology, phase selectivity and particle distribution; ↑ Easy variation and close control of the reaction parameters;	19, 53-57
	↓ Difficult to isolate large single-crystals; ↓ No easy and quick industrial implementation.	
Ultrasonic	↑ Efficient in the isolation of phase-pure materials; ↑ Homogeneous particle size and morphology in short periods of time; ↑ Suitable method for the preparation of nano-sized MOFs;	58-62
	↓ Ultrasound waves can break crystallites hindering the formation of large single-crystals for X-ray diffraction studies.	
One-pot	↑ Probably the easiest synthetic approach to prepare MOFs using ambient conditions (pressure and temperature). ↑ Possibility to increase the reaction temperature using a regular heating plate; ↑ Medium-to-low energy consumption; ↑ Possibility to isolate MOFs in short periods of time with particle size ranging from few nanometers to several hundred of	63-67

micrometers;

↓ Sometimes with poor reproducibility of the materials isolated at high temperatures and under pressure.

Table 2

Table 2 - Examples of MOFs prepared by BASF and commercially available through Sigma-Aldrich under the tradename Basolite.

<i>Well-known MOFs going to commercial trading on a large-scale basis</i>						
Commercial name	Metal centre	Organic linker (in anionic form)	Trivial name(s)	Further information		
Basolite A100	Al	Terephthalate	MIL-53	26, 205-206		
Basolite C300	Cu	1,3,5-Benzenetricarboxylate	HKUST-1, Cu-BTC, Cu ₃ (BTC) ₂ , MOF-199	204, 207		
Basolite F300	Fe	1,3,5-Benzenetricarboxylate	Fe-BTC	26		
Basolite Z1200	Zn	2-Methylimidazole	ZIF-8	207-208		
Basolite M050	Mg	Formate	–	26, 209		
<i>Other commercial names not highly cited in academic literature</i>						
Basolite M74	Mg	2,5-Dihydroxybenzene-1,4-dicarboxylate	IRMOF-74-I	210		
Basolite A520	Al	Fumarate	–	203, 211		
Basolite Z377	Zn	Benzenetribenzoate	MOF-177	212		
Basolite Z100H	Zn	Terephthalate	MOF-5, IRMOF-1	212		
Basolite Z200	Zn	2,6-Naphthalenedicarboxylate	IRMOF-8	212		

Figure 1

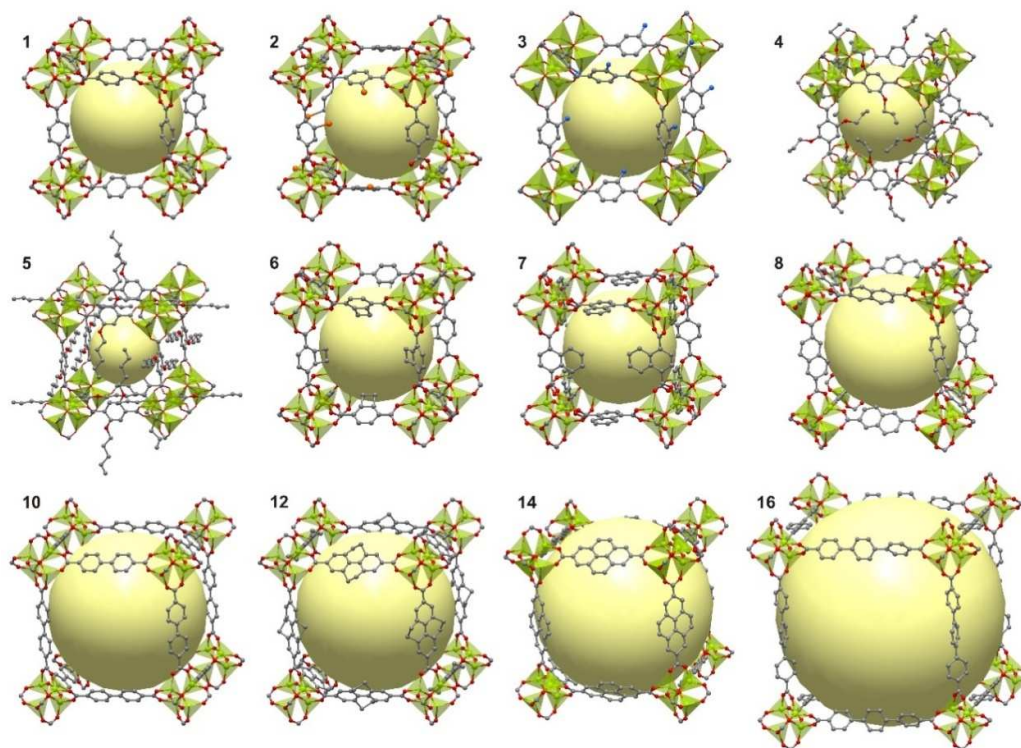


Figure 1 - Crystal structures of the porous IRMOF- n series (IRMOF = Iso-Reticular Metal-Organic Framework). Perspective view of the twelve example structures having the cubic topology of MOF-5 (also known as IRMOF-1), starting from the smallest (*left*), $n = 1$ through 7, 8, 10, 12, 14, and 16, labelled respectively. The doubly interpenetrated IRMOFs-9, 11, 13 and 15 are not represented. The IRMOFs family is prepared using organic molecules derivatized from 1,4-benzenedicarboxylic acid. The linkers differ in functionality of the pendant groups (IRMOF-1 to -7) and in length (IRMOF-8 to -16), with the later expansion resulting in the increase of the IRMOF internal void space. Zn atoms are depicted in green, O in red, C in grey, Br atoms in orange, and amino groups in blue (all hydrogen atoms have been omitted for clarity). The large yellow spheres represent the largest van der Waals spheres that can fit inside the cavities without touching the frameworks. (Adapted with permission from references ref. 14. Copyright 2002 The American Association for the Advancement of Science.)

Figure 2

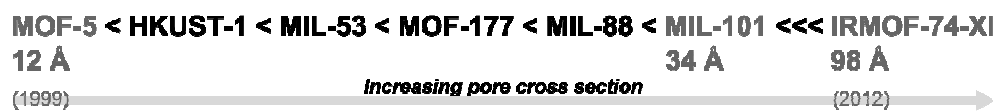


Figure 2 - Pore cross section size of the currently most-cited MOFs available in the literature. The order in which the compounds are depicted does not obey their chronological appearance in the literature but instead concern the increase in cage size. The grey bar denotes the time period since the early preparation of MOF-5 to the design of the MOF material with the higher pore size value known to date.

Figure 3

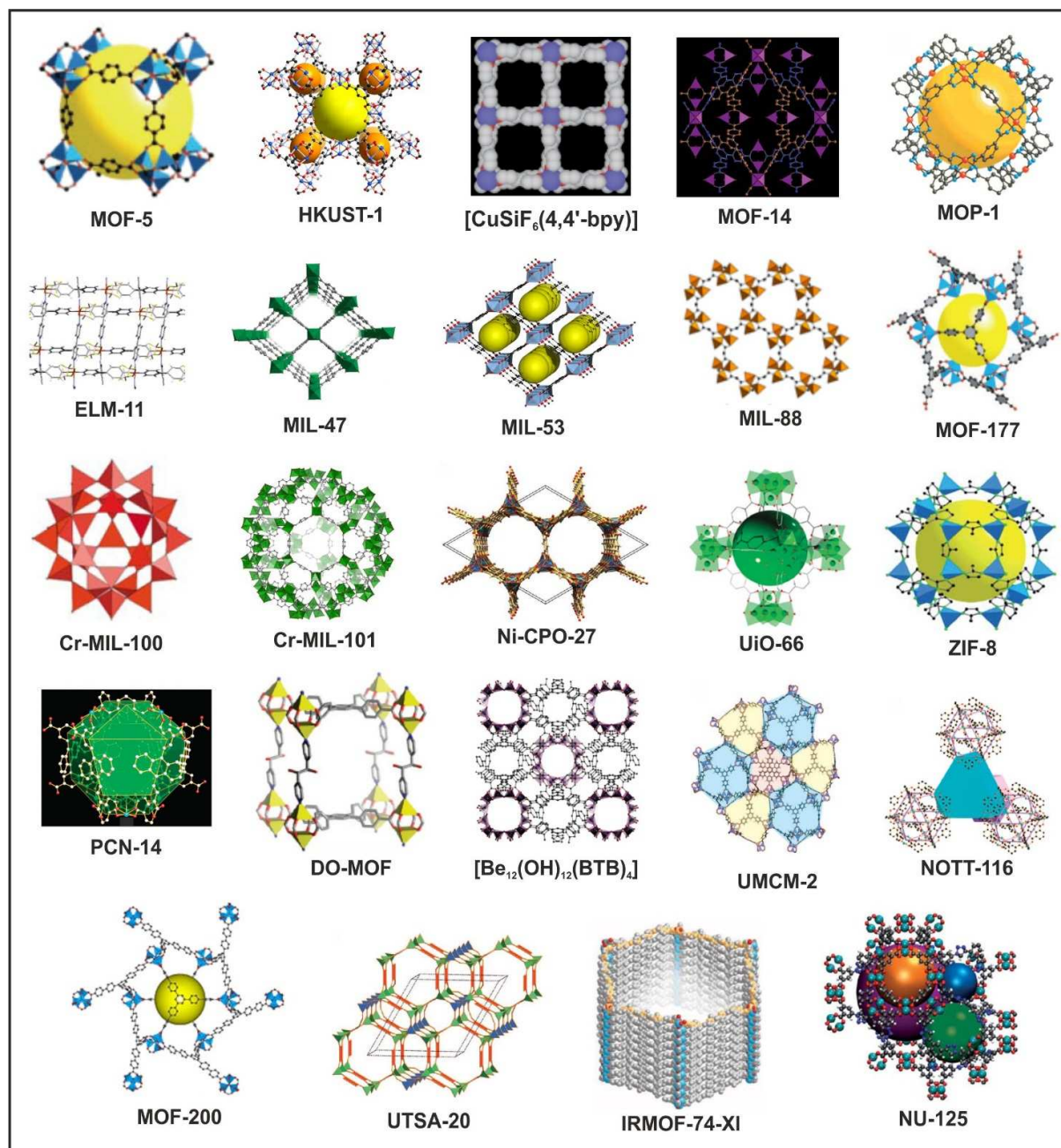


Figure 3 - Porous MOFs prepared by several research groups aiming the accommodation/retention of chemical species in their pores/channels.

Figure 4

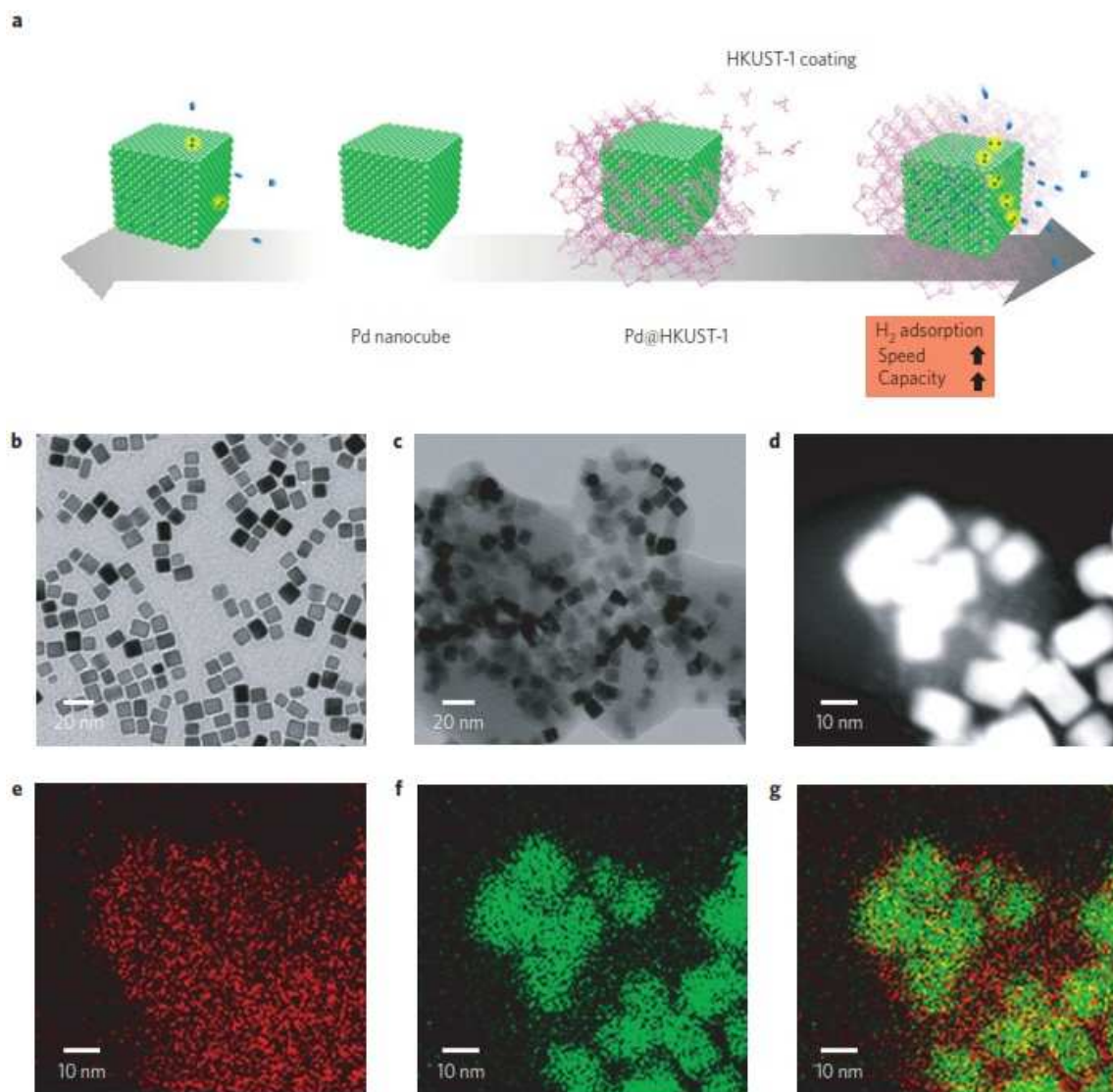


Figure 4 - (a) Schematic representation of the Pd nanocubes and Pd@HKUST-1 material used for hydrogen storage. TEM images of the (b) Pd nanoparticles and (c) Pd@HKUST-1. EDX mapping of (e) Cu, (f) Pd and (g) the overlay of the Cu and Pd elements for Pd@HKUST-1. (Reprinted with permission from ref. 96. Copyright 2014 Nature Publishing Group.)

Figure 5

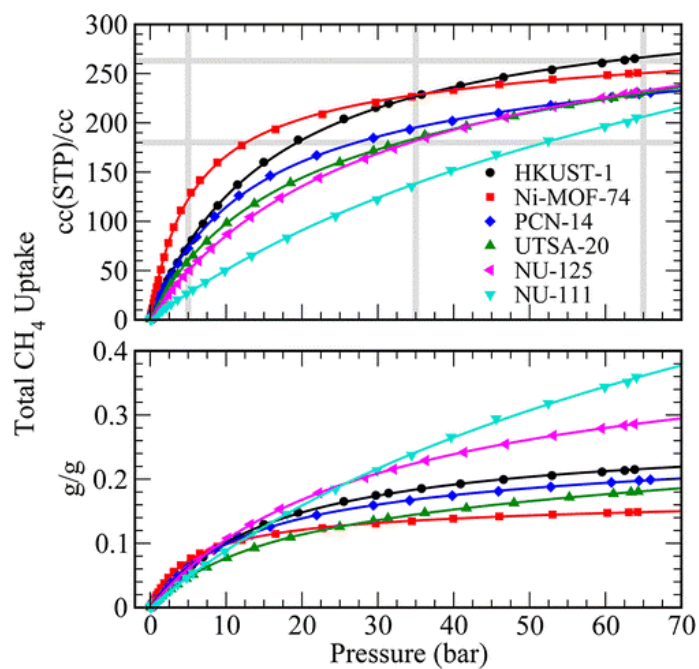


Figure 5 - Total volumetric (*top*) and gravimetric (*bottom*) CH₄ uptake for six well-known MOF materials. The old and new DOE targets for volumetric CH₄ uptake are represented as grey lines. The target gravimetric value is 0.5 g of CH₄ per gram of sorbent. (Reprinted with permission from ref. 77. Copyright 2013 American Chemical Society.)

Figure 6

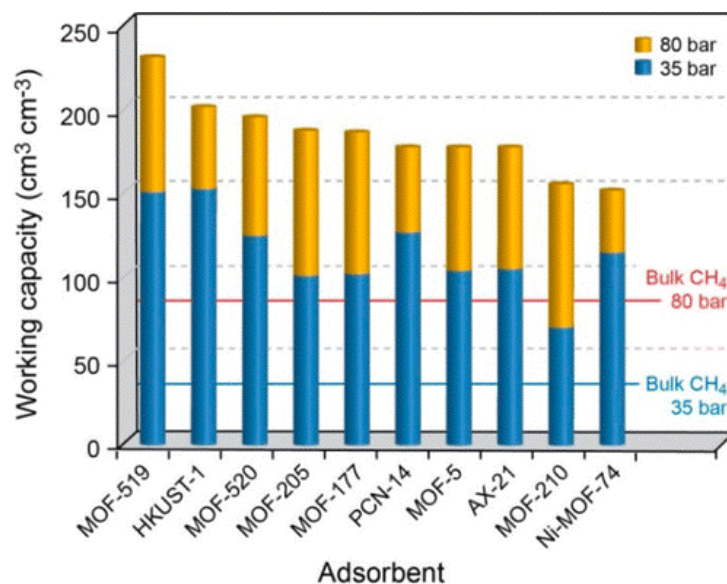


Figure 6 - Comparison between the working capacities of MOF-519 and MOF-520, and all the top-performing MOF materials plus the activated carbon AX-21. Values were determined as the differences between the uptake at 35 (blue) or 80 bar (orange) and the uptake at 5 bar. As a reference, data of the working capacity for bulk methane is overlaid. (Reprinted with permission from ref. 113. Copyright 2014 American Chemical Society.)

Figure 7

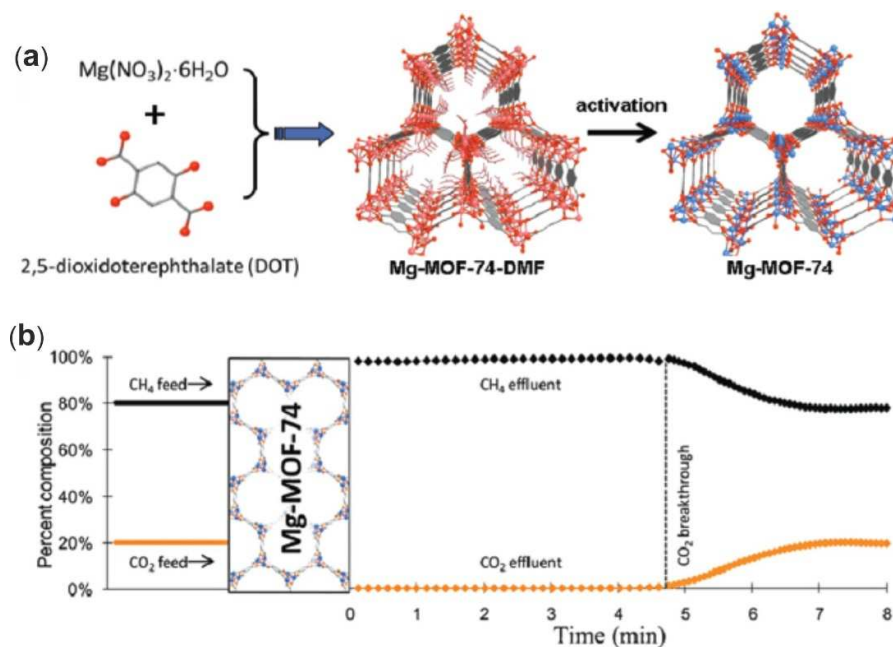


Figure 7 - (a) Schematic representation of the synthesis and structure of the as-prepared Mg-MOF-74-DMF and the activated Mg-MOF-74 materials (C = grey, O = red, terminal ligands and 6-coordinated Mg = pink and 5-coordinated Mg = blue). (b) Breakthrough curves resulting of the separation process using a mixture of CH_4/CO_2 (4:1). (Adapted with permission from ref. 129)

Figure 8

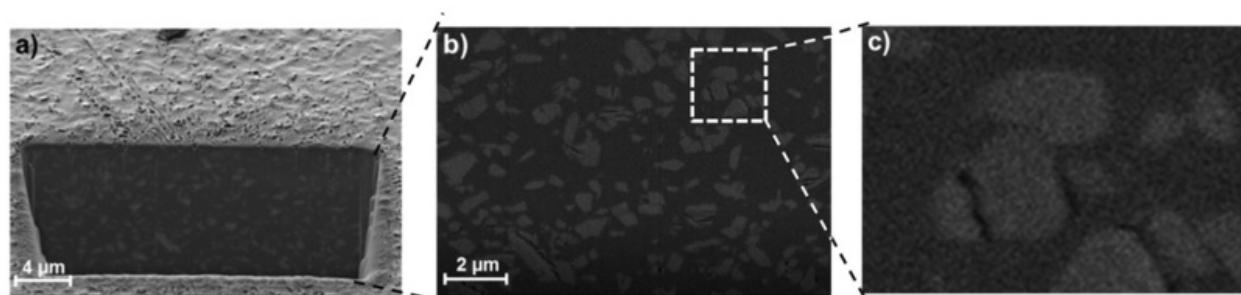


Figure 8 - FIB-SEM images of the NH₂-MIL-53(Al)/polyimide_25% membrane showing: (a) the hole created by the FIB milling of the membrane specimen; (b) a representative cross-section of the membrane in the backscattered electron (BSE) imaging mode; and (c) enlarged view of a small region represented in (b) showing the contrast difference between the matrix, the MOF filler and the inter-phase voids. (Reprinted with permission from ref. 141. Copyright 2015 Wiley-VCH.)

Figure 9

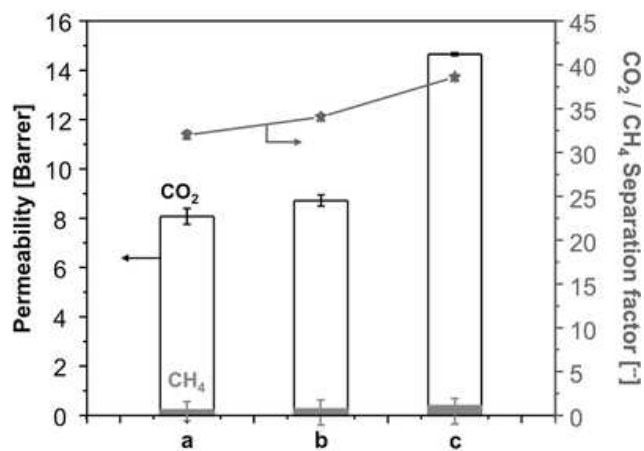


Figure 9 - CO₂/CH₄ separation performance of the NH₂-MIL-53(Al)-based membranes as a function of the MOF loading. Operation conditions: CO₂/CH₄ gas mixture = 1:1, T = 308 K, ΔP = 3 bar. Error bars represent the standard deviation. (Reprinted with permission from ref. 141. Copyright 2015 Wiley-VCH.)

Figure 10

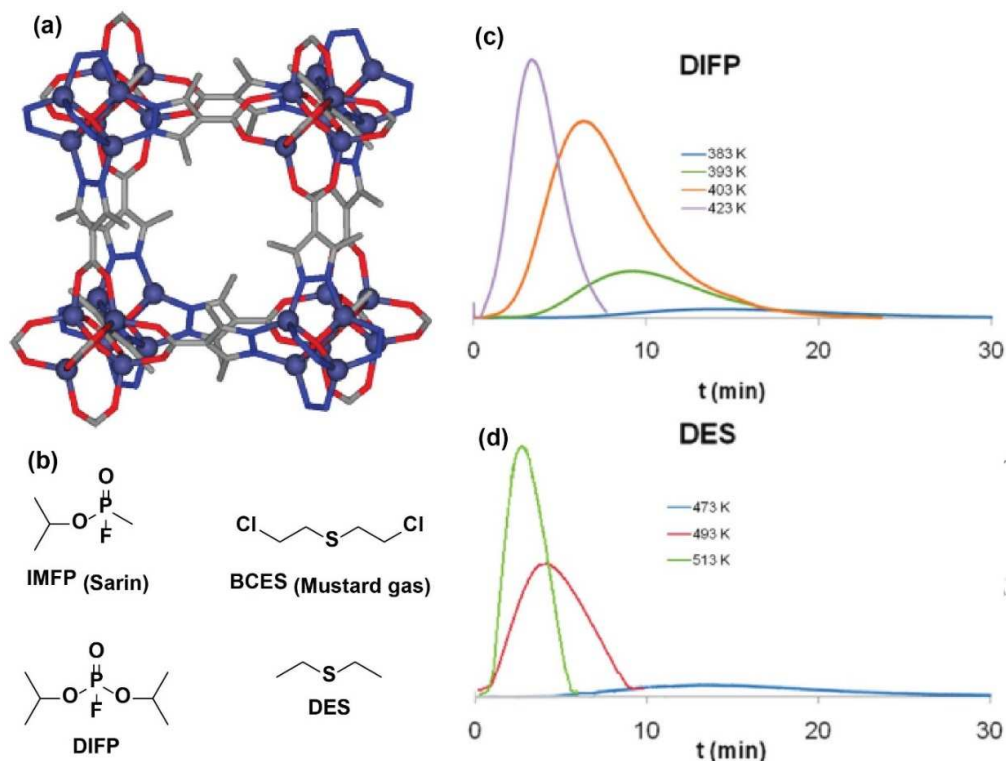


Figure 10 - (a) Perspective view of a portion of the crystal structure of $[\text{Zn}_4(\mu_4\text{-O})(\mu_4\text{-4-carboxy-3,5-dimethyl-4-carboxy-pyrazolato})_3]$ with segregated $\text{Zn}_4\text{O}(\text{CO}_2)_6$ and $\text{Zn}_4\text{O}(\text{pz})_3$ secondary building units. (b) Molecular structure of isopropylmethyl-fluorophosphate (IMFP, Sarin nerve gas) and bis(2-chloroethyl)sulfide (BCES, mustard vesicant gas) and their analogues diisopropylfluorophosphonate (DIFP) and diethylsulfide (DES), respectively, used in the study of Navarro's research group. Pulse gas chromatograms, measured at different temperatures, for (c) DIFP and (d) DES flowing through a column packed with $[\text{Zn}_4(\mu_4\text{-O})(\mu_4\text{-4-carboxy-3,5-dimethyl-4-carboxy-pyrazolato})_3]$ using a He flow of 30 mL min^{-1} . (Adapted with permission from ref. 152. Copyright 2011 American Chemical Society.)

Figure 11

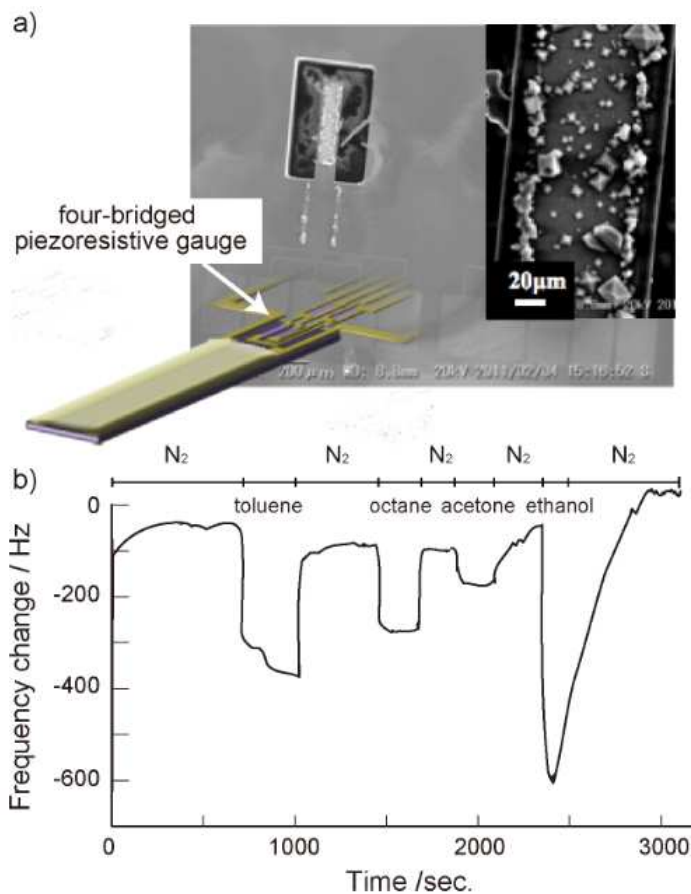


Figure 11 - (a) SEM image of [Cu₃(BTC)₂] MOF-based thin film grown from a COOH-terminated SAM on the top of gold electrode of silicon microcantilever resonator. (b) Frequency response of the MOF-based film coating the microcantilever resonator upon exposure to 100 ppm of toluene, octane, acetone and ethanol vapours. (Reprinted with permission from ref. 165. Copyright 2014 Nature Publishing Group.)

Figure 12

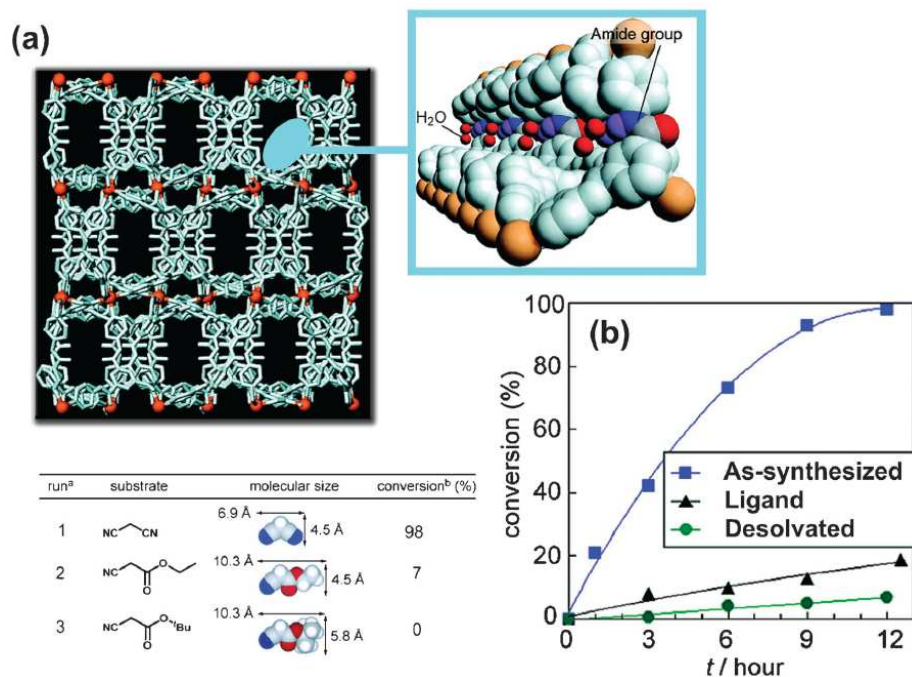


Figure 12 - (a) Crystal structure of $\{[\text{Cd}(4\text{-btapa})_2(\text{NO}_3)_2] \cdot 6\text{H}_2\text{O} \cdot 2\text{DMF}\}_n$ emphasizing the zigzag channels present in the structure. (*top right*) View of the ordered amide groups decorating the surface of the channels and interacting with water molecules *via* hydrogen bonds. Cd atoms = light brown, O atoms = red, N atoms = blue, C atoms = gray and H atoms = purple. (b) Conversion for the Knoevenagel condensation reaction of benzaldehyde with malononitrile catalyzed by the as-synthesized (blue squares) and desolvated (green circles) materials and organic ligand (black triangles). (*bottom left*) Table summarizing the results of the Knoevenagel condensation reaction for the various substrates. (Adapted with permission from ref. 173. Copyright 2007 American Chemical Society.)

Figure 13

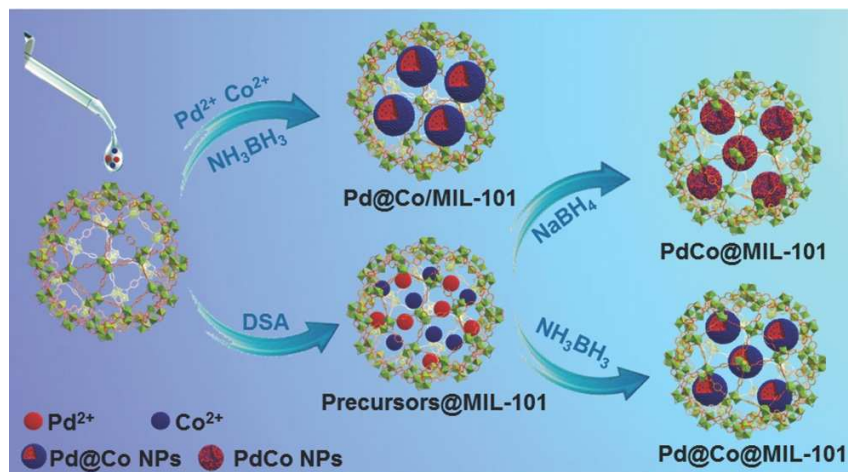


Figure 13 - Schematic representation of the preparation of the Pd@Co/MIL-101, PdCo@MIL-101 and Pd@Co@MIL-101 catalysts using different synthetic methodologies and reducing agents. (Reprinted with permission from ref. 180. Copyright 2015 Wiley-VCH.)

Figure 14

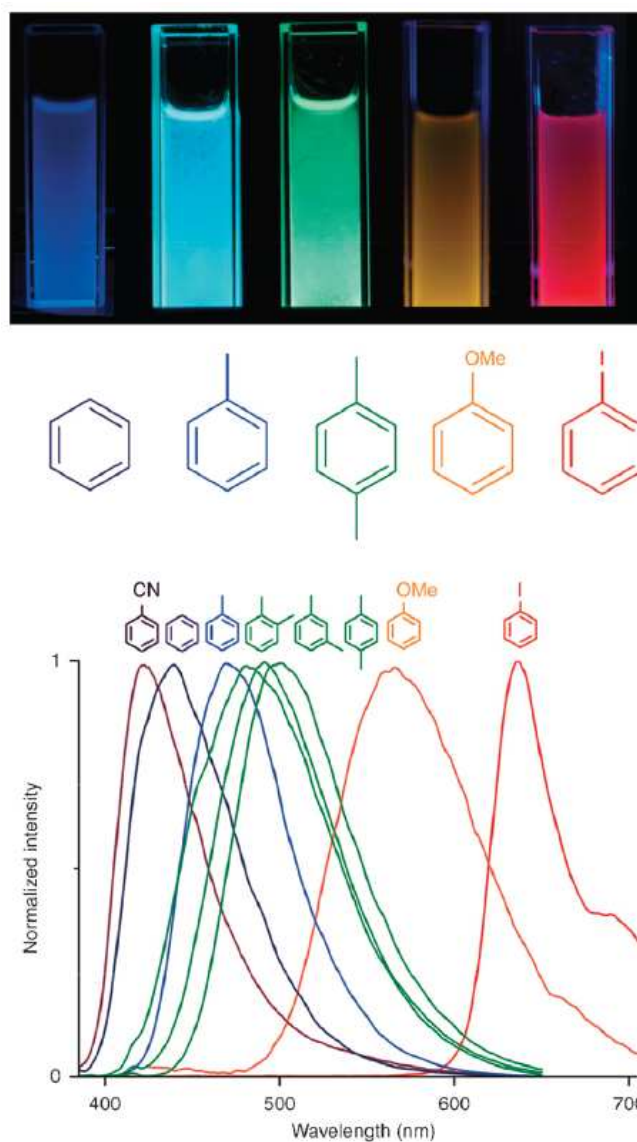


Figure 14 - (top) Luminescence of the powdered $[\text{Zn}_2(\text{bdc})_2(\text{dpNDI})]_n$ material suspended in aromatic VOC liquids, with the corresponding structures below, after excitation at 365 nm using a commercial ultraviolet lamp. (bottom) Collected normalized spectra of the $[\text{Zn}_2(\text{bdc})_2(\text{dpNDI})]_n > \text{VOC}$ compounds excited at 370 nm. (Adapted with permission from ref. 194. Copyright 2011 Macmillan Publishers Limited.)

Figure 15

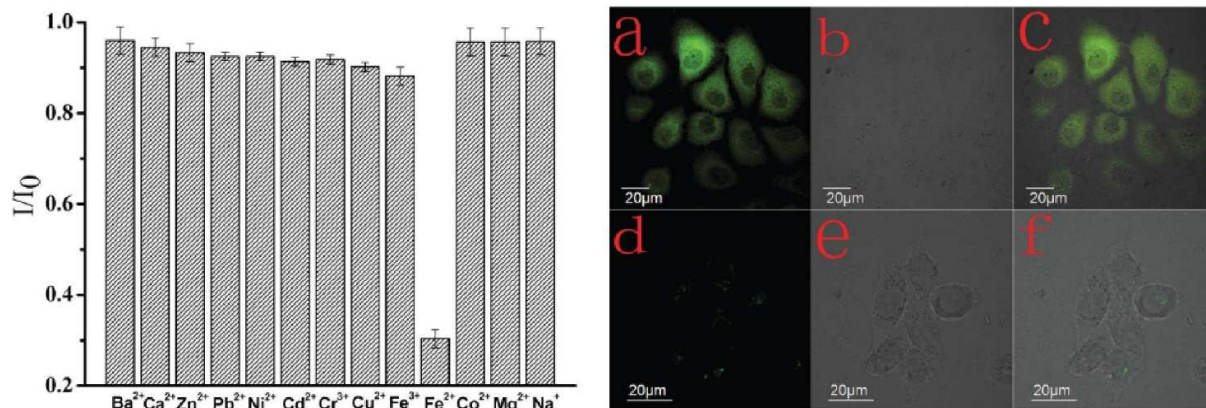


Figure 15 - (left) Comparison of the fluorescence intensity of different metal cations interacting with the MOF-253 (γ) material (50 mg L^{-1}) activated in $100 \mu\text{M M}^{x+}$ ($x = 1, 2$ or 3) aqueous solution. I and I_0 correspond to the fluorescence intensity of MOF-253 (γ) with and without metal cations, respectively. (right) Confocal fluorescence and brightfield images of the HeLa cells: (a) fluorescent, (b) brightfield and (c) overlay images of HeLa cells marked with $5 \mu\text{M}$ of MOF-253 (γ) at $37 \text{ }^\circ\text{C}$ during 3 h; (d) fluorescent, (e) brightfield and (f) overlay images of HeLa cells incubated, at $37 \text{ }^\circ\text{C}$ for 1 h, with $5 \mu\text{M}$ of MOF-253 (γ) and then supplemented with $50 \mu\text{M}$ of FeCl_2 in the growth media ($\lambda_{\text{ex}} = 405 \text{ nm}$). (Adapted with permission from ref. 190. Copyright 2014 Royal Society of Chemistry.)

Figure 16

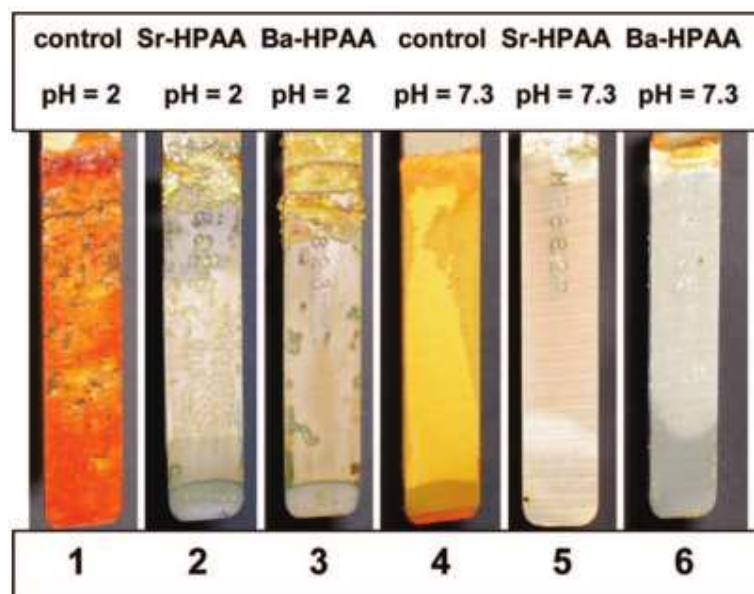


Figure 16 – Anticorrosion effect of Sr-HPAA and Ba-HPAA films on carbon steel specimens at pH 2.0 and 7.3. Corrosion inhibition induced by the generated metal-HPAA films is evident (specimens **2**, **3**, **5** and **6**) when compared with the “control” (specimens **1** and **4**). Specimens **2** and **3** (pH 2.0) are free of iron oxide, however, corrosion rates are higher than that of the “control”. (Reprinted with permission from ref. 75. Copyright 2008 American Chemical Society.)

Figure 17



Figure 17 – Large-scale production of MOFs at BASF facilities in Germany. Image credit: BASF. (Reprinted with permission from ref. 219)

Figure 18

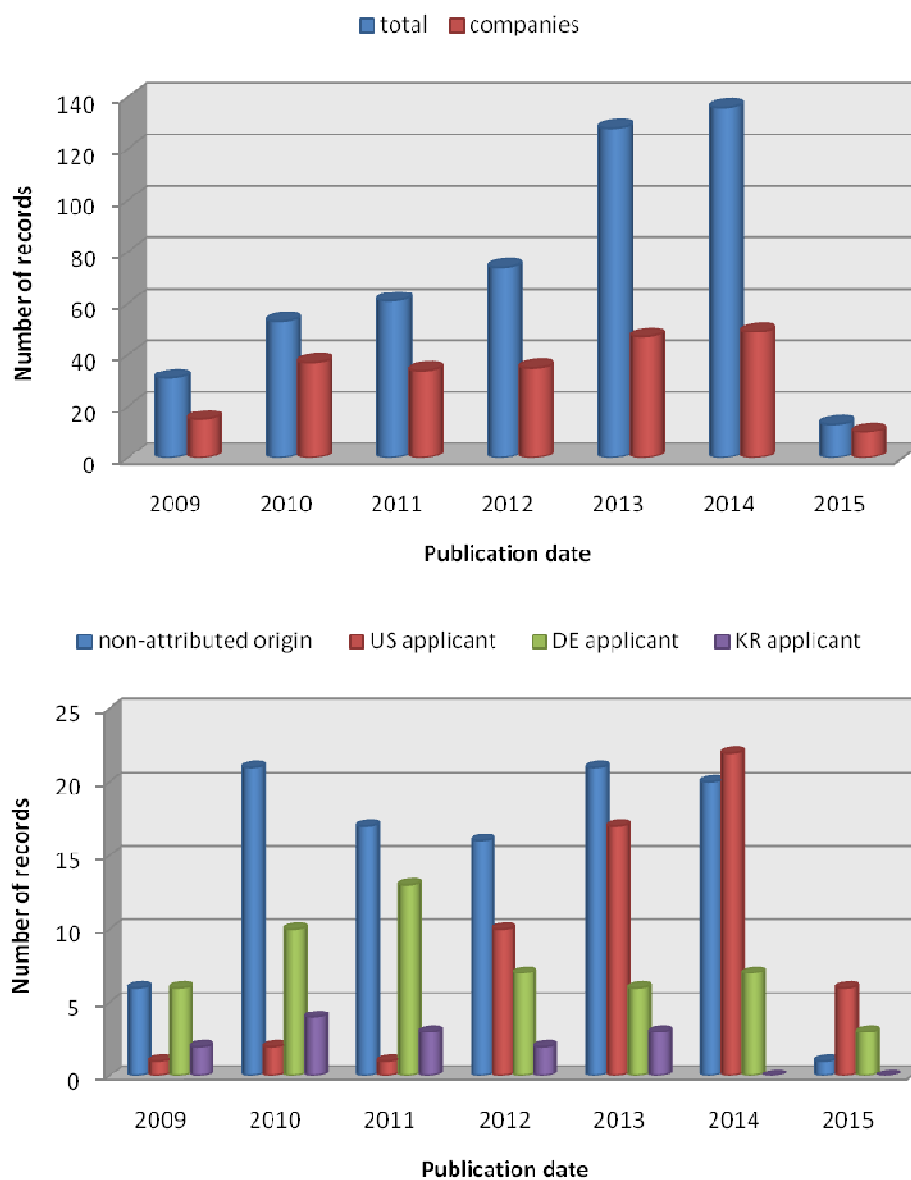


Figure 18 – The most recent patent publications according to the European Patent Office database. Search Terms (in the title or abstract): Metal-Organic Framework; Worldwide collection (90+ countries); Limited to the last 7 years. (*Top*) Blue stands for the total number of patents filed, and red for the number of patents solely filed by companies. (*Bottom*) Geographical distribution of the patents solely filed by companies: red for United States of America, green for Germany, purple for South Korea, and blue for those whose origin was not directly attributed by the query results.

Figure 19

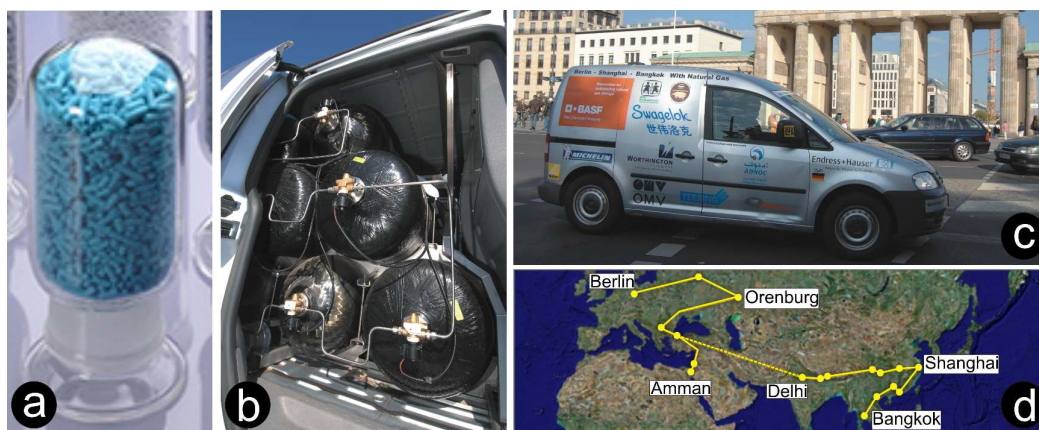


Figure 19 – EcoFuel Asia Tour 2007 - Berlin to Bangkok: 32 000 km with Basolite C300 in tank. **(a)** Basolite C300 (HKUST-1); **(b)** MOF-enhanced fuel tanks with CH₄; **(c)** Volkswagen Caddy EcoFuel prototype car; **(d)** journey map. (Adapted with permission from ref. 202)

Figure 20

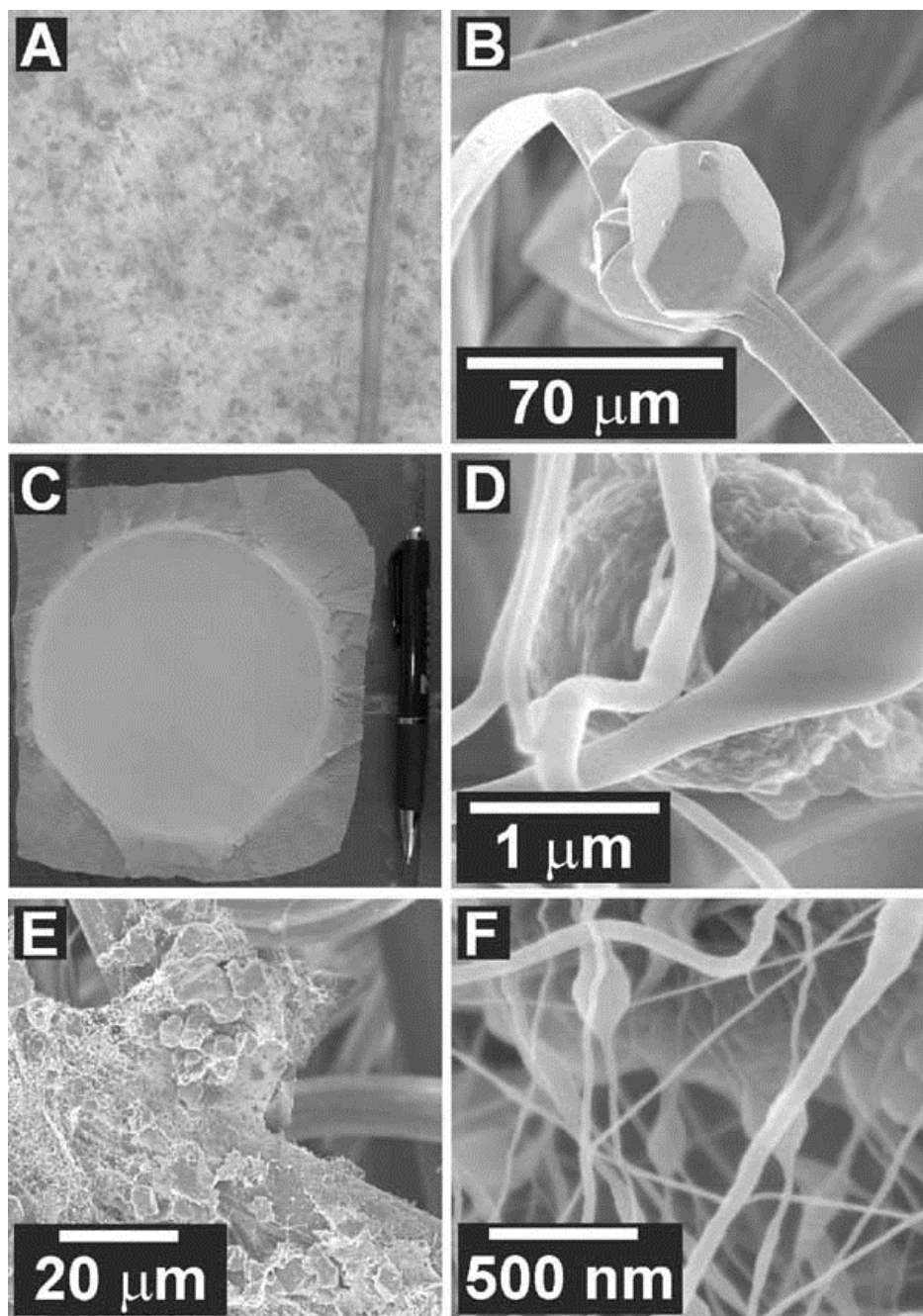


Figure 20 – Images (A and C) and SEM micrographs (B, D, E and F) from electrospun MOF/fiber composites: (A) HKUST-1/polystyrene (PS) fibers compared to a human hair; (B) HKUST-1 crystal on a PS fiber analogue to a pearl necklace; (C) homogeneous MIL-100(Fe)/polyvinylpyrrolidone (PVP) layer on polypropylene non-woven; (D) MIL-100(Fe) particle in PVP fiber web; (E and F) HKUST-1 particles (BASF) in polyacrylonitrile (PAN) fibers on a PAN non-woven (large substrate fibers in the background). (Reprinted with permission from ref. 242. Copyright 2011 Wiley-VCH.)

Figure 21



Figure 21 – Continuous and large-scale production process developed by Norafin in the context of NanoMOF project (reference FP7-NMP-2008-LARGE-2). (*Top left*) Principle of the dry loading process and (*top right*) the scattering-suction unit. (*Bottom*) Continuously MOF-particle loaded PET-nonwovens (HKUST-1 <math><63\ \mu\text{m}</math> from Johnson Matthey company; loading capacity: 25 g/m²). [Reprinted from http://cordis.europa.eu/project/rcn/92877_en.html (accessed 02 March 2015).]

Figure 22

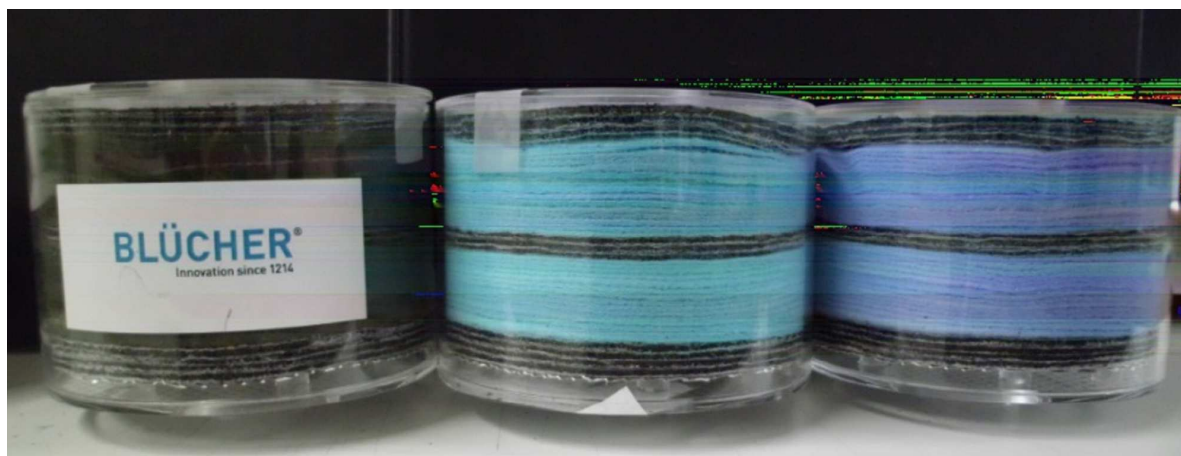


Figure 22 – Examples of filter canisters after the breakthrough test with cyclohexane, NH_3 and H_2S (from right to left). The change in colour of the MOF particles (mainly for cyclohexane and H_2S) is an indicator for the adsorption of the test gases. NanoMOF project (reference FP7-NMP-2008-LARGE-2). [Reprinted from http://cordis.europa.eu/project/rcn/92877_en.html (accessed 02 March 2015).]